

AD-A061 717

AIR FORCE GEOPHYSICS LAB HANSCOM AFB MASS

F/G 4/1

PRECEDE II: SUMMARIZED RESULTS OF AN ARTIFICIAL AURORAL EXPERIM--ETC(U)

MAR 78 R R O'NEIL

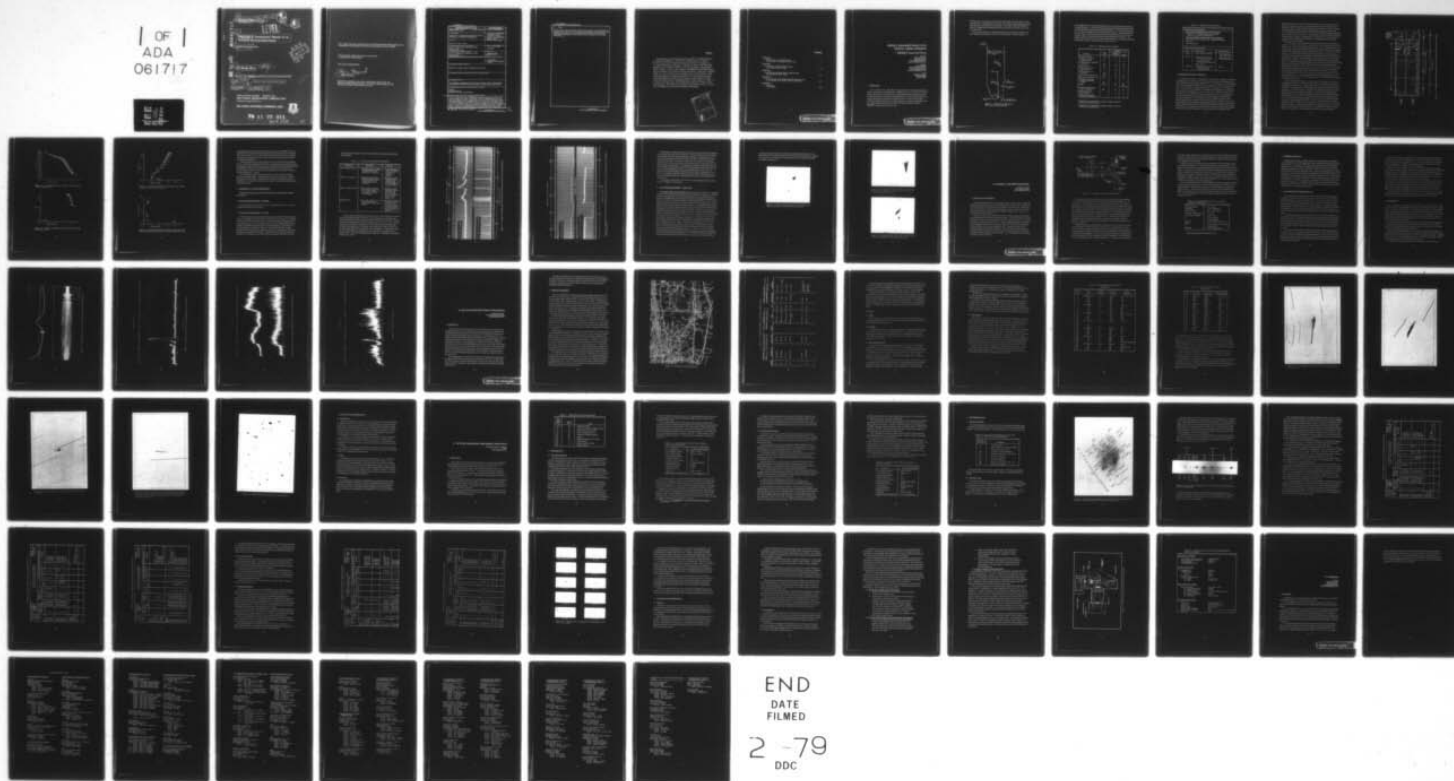
UNCLASSIFIED

AFGL-TR-78-0063

DNA-HAES-77

NL

1 OF 1
ADA
061717



END
DATE
FILMED

2-79
DDC

ADA061717

DDC FILE COPY

14

AFGL-TR-78-0063, AFGL-ERP-627

9

ENVIRONMENTAL RESEARCH PAPERS NO. 627
HAES REPORT NO. 77

15



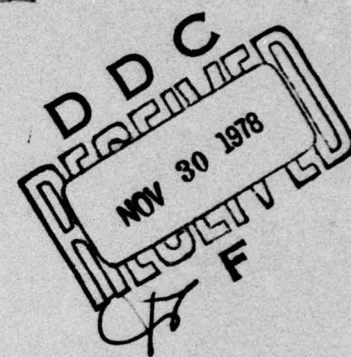
LEVEL

6

**PRECEDE II Summarized Results of an
Artificial Auroral Experiment,**

10

ROBERT R. O'NEIL Editor



11

16 March 1978

12 74p.

16

7670

This research was supported by the Defense Nuclear Agency under Subtask L25AAXHK632 entitled "IR Phenomenology and Optical Code Data Base."

17

10, X632

Approved for public release; distribution unlimited.

18

DNA

19

HAES-77

627104
62101

OPTICAL PHYSICS DIVISION PROJECT 7670
AIR FORCE GEOPHYSICS LABORATORY
HANSOM AFB, MASSACHUSETTS 01731

AIR FORCE SYSTEMS COMMAND, USAF



78 11 27 011

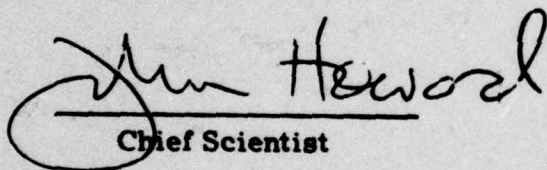
409 578

LB

This report has been reviewed by the ESD Information Office (OI) and is releasable to the National Technical Information Service (NTIS).

This technical report has been reviewed and is approved for publication.

FOR THE COMMANDER


Chief Scientist

Qualified requestors may obtain additional copies from the Defense Documentation Center. All others should apply to the National Technical Information Service.

Unclassified

SECURITY CLASSIFICATION OF THIS PAGE (When Data Entered)

REPORT DOCUMENTATION PAGE		READ INSTRUCTIONS BEFORE COMPLETING FORM
1. REPORT NUMBER AFGL-TR-78-0063 ✓	2. GOVT ACCESSION NO.	3. RECIPIENT'S CATALOG NUMBER
4. TITLE (and Subtitle) PRECEDE II: SUMMARIZED RESULTS OF AN ARTIFICIAL AURORAL EXPERIMENT		5. TYPE OF REPORT & PERIOD COVERED HAES Report No. 77 ✓ Scientific. Interim.
7. AUTHOR(s) Robert R. O'Neil, Editor		6. PERFORMING ORG. REPORT NUMBER ERP no. 627 ✓ 8. CONTRACT OR GRANT NUMBER(s)
9. PERFORMING ORGANIZATION NAME AND ADDRESS Air Force Geophysics Laboratory (OPR) Hanscom AFB, Massachusetts 01731		10. PROGRAM ELEMENT, PROJECT, TASK AREA & WORK UNIT NUMBERS 76701006
11. CONTROLLING OFFICE NAME AND ADDRESS Air Force Geophysics Laboratory (OPR) Hanscom AFB, Massachusetts 01731		12. REPORT DATE 16 March 1978 13. NUMBER OF PAGES 88
14. MONITORING AGENCY NAME & ADDRESS (if different from Controlling Office)		15. SECURITY CLASS. (of this report) Unclassified 15a. DECLASSIFICATION/DOWNGRADING SCHEDULE
16. DISTRIBUTION STATEMENT (of this Report) Approved for public release; distribution unlimited.		
17. DISTRIBUTION STATEMENT (of the abstract entered in Block 20, if different from Report)		
18. SUPPLEMENTARY NOTES This research was supported by the Defense Nuclear Agency under subtask L25AAXHX632 entitled "IR Phenomenology and Optical Code Data Base".		
19. KEY WORDS (Continue on reverse side if necessary and identify by block number) Aurora Artificial aurora Rocketborne electron accelerators		
20. ABSTRACT (Continue on reverse side if necessary and identify by block number) On 13 December 1977, PRECEDE II was launched from the White Sands Missile Range, New Mexico at 05:49:59.116 UT. PRECEDE II is one of a series of artificial auroral experiments in the DNA-AFGL EXCEDE program using pulsed high-power rocketborne electron accelerators operating in the 80- to 140-km altitude range. This launch was designed to serve as an engineer- ing test of an electron accelerator module providing a pulsed 3-kV, 7-A electron beam, to provide an engineering test for a newly designed liquid nitrogen cooled rocketborne infrared Michelson interferometer, and to observe the		

DD FORM 1 JAN 73 1473 EDITION OF 1 NOV 65 IS OBSOLETE

Unclassified

SECURITY CLASSIFICATION OF THIS PAGE (When Data Entered)

Unclassified

SECURITY CLASSIFICATION OF THIS PAGE(When Data Entered)

20. (Cont)

ultraviolet and visible emissions induced in the night sky by the rocketborne electron source with a number of ground based imaging, spectrographic, and photometric instruments. This report briefly describes the scope of the PRECEDE II experiment and summarizes the performance of the various instruments.

Unclassified

SECURITY CLASSIFICATION OF THIS PAGE(When Data Entered)

Preface

The field efforts of the following personnel in support of the PRECEDE launch is gratefully acknowledged: D. Newell and J. LaSpina of AFGL; F. Riebeck, M. Smith, and G. Ware of Utah State University; R. Marks, R. Andersen, and F. Tracy of Northeastern University; L. Briggs and P. Moriss of the White Sands Missile Range; P. Guthrie of STADS; Lt. Col. Jeas and Major J. Dunkle of ESD AFSC; W. Krag, J. Sorvari, and D. Beatty of the GEODSS facility at WSMR Stallion site; R. Bergemann and D. Batman of Lincoln Laboratory; A. Tuttle and J. Loguidice of HSS, Inc., and D. Montoya and his colleagues of the Land Air Division of Dyna-electron who operated the optical tracking mounts in a most cooperative manner. Technical suggestions and guidance in the approach and instrumentation development in this experiment were contributed by Major J. Mayo of DNA, A.T. Stair, Jr., J. Ulwick, E.R. Huppi, and J. Rex of AFGL and K. Baker and D. Baker of Utah State University. The efficiency and assistance of Ms. Gloria Foss and C.P. Dolan, Jr. in the preparation of this report is gratefully acknowledged.

ACCESSION for	
NTIS	Write Section <input checked="" type="checkbox"/>
DDC	8 ft Section <input type="checkbox"/>
UNCLASSIFIED	
J S I R E F Y	
BY DISTRIBUTION/AVAILABILITY CODES	
DATE	FILE
AT	

Contents

CHAPTER 1

PRECEDE II: Summarized Results

R. R. O'Neil, E. McKenna, and D. Burt

7

CHAPTER 2

Rocketborne LN_2 SWIR Interferometer

J. C. Kemp and R. J. Huppi

23

CHAPTER 3

Hotel Site Ground Based Optical Measurements

W. Boquist and R. W. Deuel

33

CHAPTER 4

SE 70 Site Ground Based Spectrographic Measurements

D. F. Hansen, M. P. Shuler, and L. B. Woolaver

47

CHAPTER 5

Conclusions

R. R. O'Neil

69

PRECEDE II: SUMMARIZED RESULTS OF AN ARTIFICIAL AURORAL EXPERIMENT

1. PRECEDE II: Summarized Results

R.R. O'Neil
Radiation Effects Branch
Optical Physics Division
Air Force Geophysics Laboratory
Hanscom AFB, Massachusetts 01731

E. McKenna
Rocket Probe Branch
Aerospace Instrumentation Division
Air Force Geophysics Laboratory
Hanscom AFB, Massachusetts 01731

D. Burt
Space Science Laboratory
Utah State University
Logan, Utah 84322

1. INTRODUCTION

On 13 December 1977, PRECEDE II was launched from the White Sands Missile Range, New Mexico at 05:49:59.116 UT. PRECEDE II is one of a series of artificial auroral experiments in the DNA-AFGL EXCEDE program using pulsed high power rocketborne electron accelerators operating in the 80- to 140-km altitude range. This launch was designed to serve as an engineering test of an electron accelerator module providing a pulsed 3-kV, 7-A electron beam, to provide an engineering test for a newly designed liquid nitrogen cooled rocketborne infrared Michelson

(Received for publication 15 March 1978)

interferometer, and to observe the ultraviolet and visible emissions induced in the night sky by the rocketborne electron source with a number of ground based imaging, spectrographic, and photometric instruments. This report briefly describes the scope of the PRECEDE II experiment and summarizes the performance of the various instruments.

The projected trajectory of the Nike Aerobee 170 rocket and the location of the three optical ground stations, Hotel, SE 70, and Stallion, is shown in Figure 1-1.

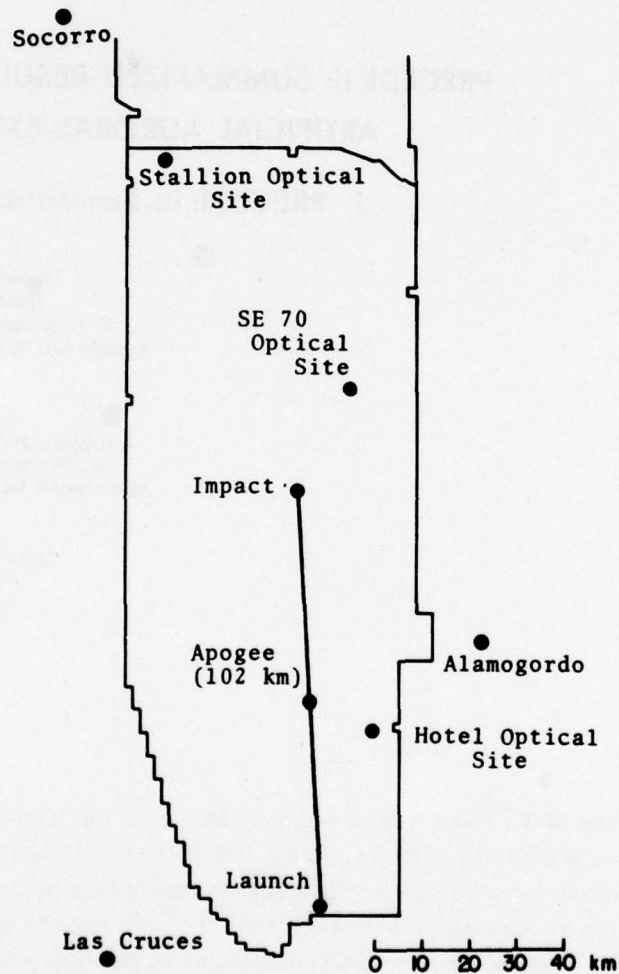


Figure 1-1. PRECEDE II Experiment:
White Sands Missile Range Map

The preflight estimate and actual altitudes of the various experiment functions are reviewed in Table 1-1. The principal rocket and ground based instrumentation utilized in the PRECEDE II experiment is summarized in Table 1-2. The payload was despun to a roll rate of approximately 0.16 revolutions per second. At approximately 264 sec after launch, the forward payload section was separated from the electron accelerator and the rocket and the forward section successfully recovered. The forward payload section consisted of the liquid nitrogen (LN_2) cooled interferometer, the telemetry section, and the parachute recovery system.

Table 1-1. PRECEDE Timer Functions

Function	Time (sec)	Altitude	
		Preflight Estimate	Actual
Sustainer Burnout	49.5	34	32
Command Closure of Engine Valves	54	40	37
Interferometer Calibration Lamp On	55.1	41	38
Despin Vehicle	69	56	52
Start Interferometer Mirror Scan	71.1	58	54
Interferometer Cap Removed	90.3	76	71
Eject Clamshell Nose Tip	92.7	79	73
Removed Accelerator Door	105.7	88	82
Energize Accelerator Filaments and High Voltage	108.1	90	83
Apogee	179.6	114	102 (172 sec)
Separate Interferometer from Accelerator	264	80	62
Stop Interferometer Mirror Scan*		15	15
Deploy Interferometer Recovery Parachute**		5	5

* This function is initiated by a pressure sensitive switch at 50,000 ft on payload descent.

** This function is initiated by a pressure sensitive switch at 15,000 ft on payload descent.

Table 1-2. PRECEDE II Instrumentation

Rocketborne Instrumentation		
<u>Non Recovered Payload Section, 38-cm diameter</u>		
21-kW (3-kV, 7-A) pulsed electron accelerator, length 91 cm, weight 160 kilograms		
<u>Recovered Nosetip Payload Section, 30-cm diameter</u>		
LN ₂ interferometer, length 61 cm, weight 40 kilograms		
Telemetry		
Recovery System		
Ground Based Instrumentation		
Site	Instruments	Tracking Mode
Hotel	Film and video cameras	Radar controlled automatic mount
SE 70	Dual channel, 3914 and 5577A telephotometer UV and visible image intensified spectrographs	Radar controlled automatic mount
Stallion	Film camera GEODSS satellite tracking telescope and video recording system	Manual

2. ROCKETBORNE ELECTRON ACCELERATOR

The electron accelerator, constructed by D. Burt and F. Riebeek of Utah State University, was a variation on the design successfully used on the PRECEDE I and EXCEDE:SWIR artificial auroral experiments. The accelerator, 38-cm in diameter, 91-cm long and weighing 160 kilograms, was designed to provide a nominal 20 kW beam of 3 kV electrons. A pulse period of 6 sec, composed of a 4.3 sec beam on and a 1.7 sec beam off component, was intended to be repeated for the duration of the experiment, anticipated to be on the order of 3 min assuming nominal rocket performance. The PRECEDE II launch was designed, in part, as an engineering test of a prototype electron accelerator module to be used on the subsequent EXCEDE II experiment. The accelerator used two tungsten filaments directly heated to approximately 2800°K; electron acceleration was provided by nickel cadmium batteries which constituted the principal accelerator weight. The accelerator design included a latchout relay circuit which shut off the accelerator high voltage for periods of up to several sec in the event the current drain from the high voltage battery pack exceeded 10 amperes. The latch out relay was intended to avoid

catastrophic failure by limiting the energy dissipated if the accelerator operated briefly in a short circuit mode. Previous experience in both a rocket test and laboratory vacuum chamber studies with electron accelerators of similar cathode anode configuration indicated high voltage breakdown and short circuit arcing occurred if the gas pressure of an air-like mixture within the accelerator assembly was in excess of several milli-Torr. The accelerator cathode anode assembly was vacuum sealed, evacuated, and heated prior to assembly on the rocket vehicle to minimize excess accelerator gas density due to outgassing when the tungsten filaments were initially heated.

The accelerator door was opened, filaments heated and high voltage applied (Table 1-1) by 108 sec after launch. Altitude at this time was approximately 83 km, somewhat less than the preflight estimate of 90 km. The accelerator operated in an arcing mode, high voltage breakdown within the accelerator structure, for approximately 30 sec until the payload achieved an altitude of 97 km at 138 sec after lift off (Figure 1-2). During the arcing mode, the latch out protection circuit limited the maximum energy dissipation and prevented catastrophic failure due to fusing of any accelerator components. At approximately 138 sec after launch, the accelerator produced a 4.3 sec pulse of 3 kV electrons depositing 20 kW into the night atmosphere. As indicated in subsequent sections of this report, the electron induced ultraviolet and visible emissions were readily recorded by the ground based optical instruments. As shown in Figures 1-3, 1-4, and 1-5, the accelerator power output showed slight loading characteristics during a given pulse and the power output decreased from approximately 20 kW at 138 sec after launch (97 km on payload ascent) to approximately 13 kW at 212 sec (95 km on payload descent). At lower descent altitudes, the accelerator continued operation, pulsing sporadically and providing an electron beam of several kilowatts to a descent altitude of approximately 64 km (see Figure 1-6).

The accelerator performance reviewed in Figures 1-2 through 1-6 is based on the rocketbased monitors of accelerator voltage and current telemetered with other rocketbased measurements. At 264 sec after launch the accelerator and Aerobee 170 rocket were separated from the payload section containing the interferometer, telemetry, and recovery system. Although the rocketbased monitors of accelerator performance were no longer telemetered, the ground based telephotometer indicated the electron accelerator operated in an arcing mode at descent altitudes less than 64 km. The electron accelerator functioned well, without arcing, from 97 km on payload ascent through apogee (102 km) until 81 km on payload descent, a period of approximately 100 seconds. The accelerator operated somewhat sporadically for an additional 43 sec depositing a final pulse of 3 kV electrons into the atmosphere at 64 km on payload descent. Intermittent arcing at the lower altitudes during payload ascent and descent is consistent with similar effects observed in laboratory vacuum chamber studies at higher gas densities.

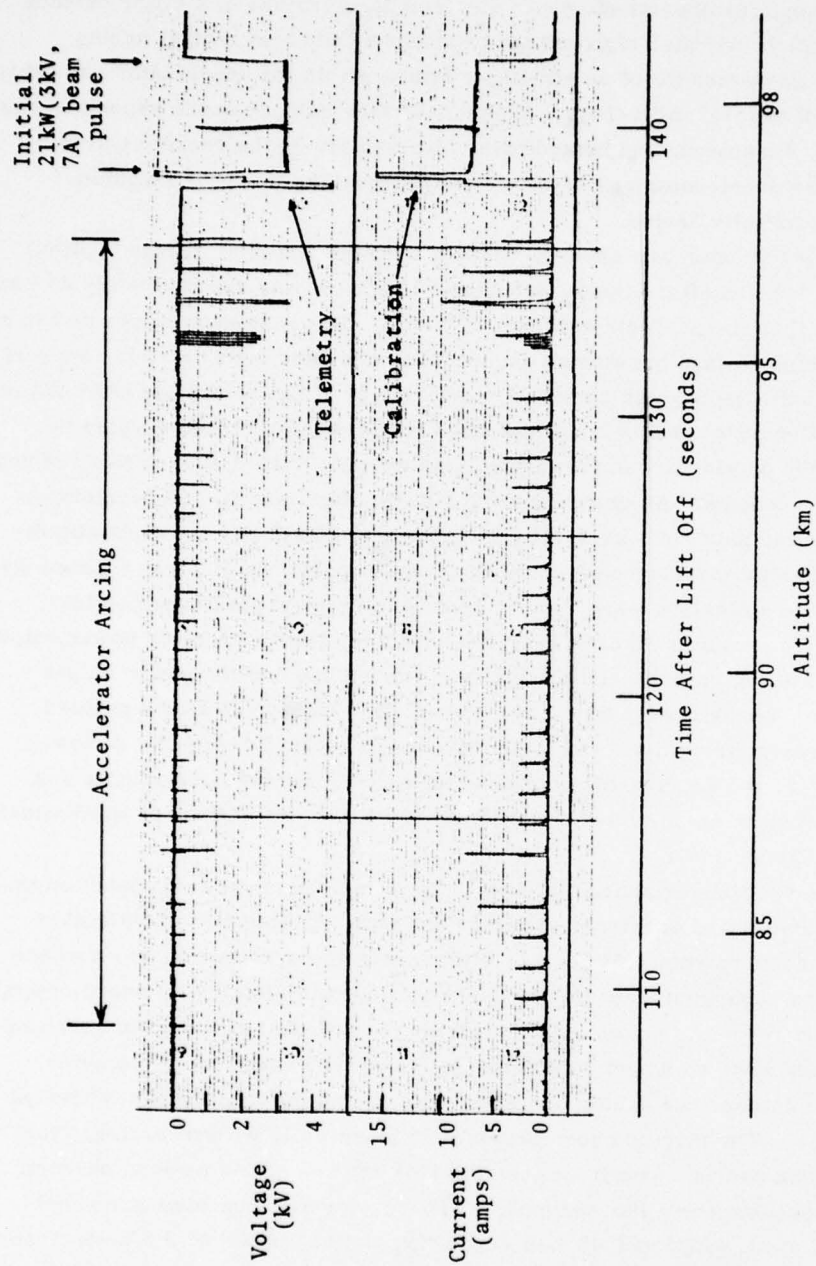


Figure 1-2. Telemetered Rocketborne Monitors of Accelerator Beam Current and Voltage

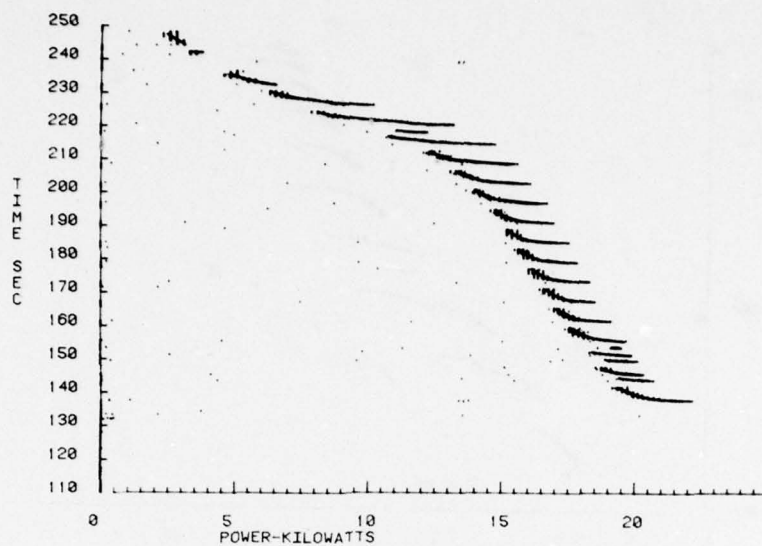


Figure 1-3. Telemetered Monitor of Electron Accelerator Beam Power, Flight Summary

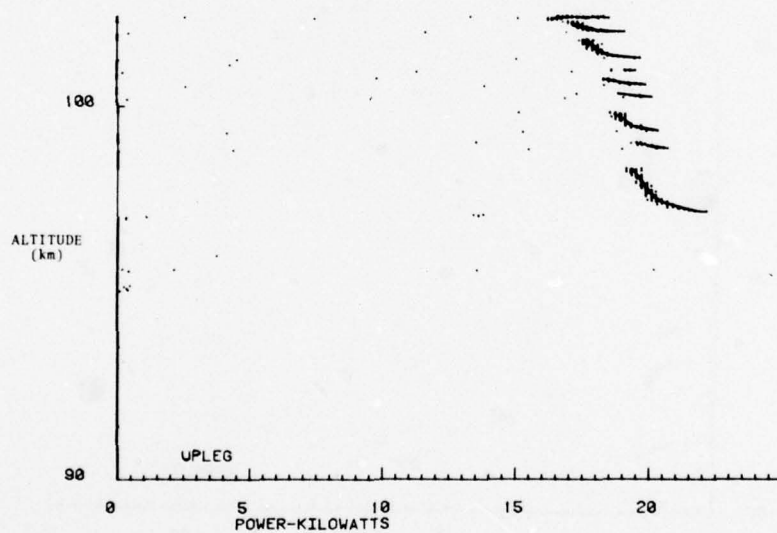


Figure 1-4. Telemetered Monitor of Accelerator Power During the Payload Ascent

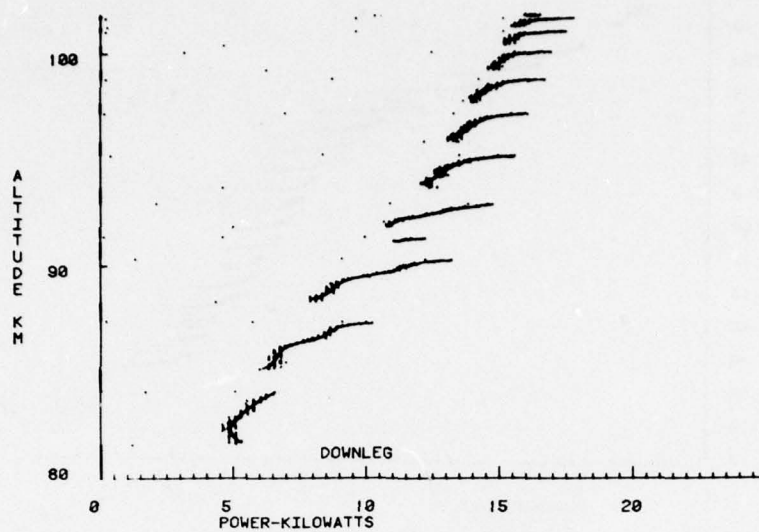


Figure 1-5. Telemetered Monitor of Accelerator Power During the Initial Portion of Payload Ascent

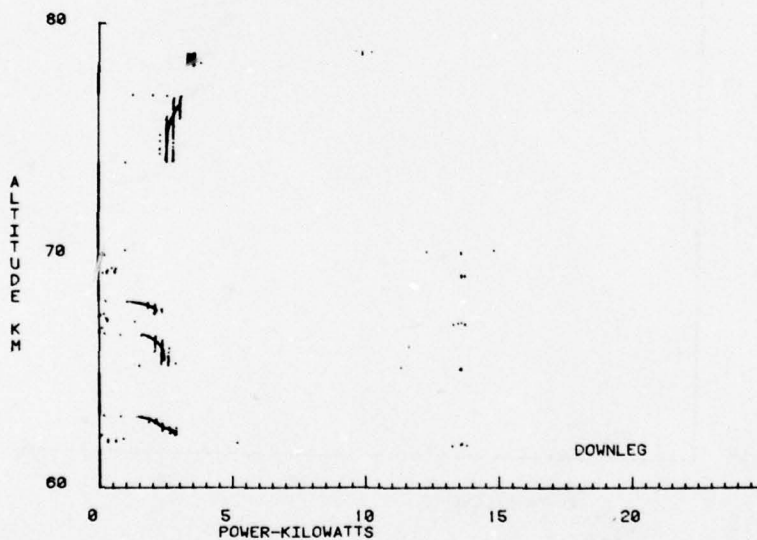


Figure 1-6. Telemetered Monitor of Electron Accelerator Beam Power During the 80 to 60 km Altitude Range on Payload Descent

During flight the gas density within the accelerator cavity is controlled by the combined effects of ambient atmospheric density, the density enhancement or reduction due to the so-called "ram" or "wake" effect as determined by the cavity orientation with respect to the payload velocity vector and finally any significant accelerator assembly outgassing effects.

Continued production of an electron beam at the low descent altitudes suggests that the arcing observed between 83 and 97 km on payload ascent was caused in part by outgassing of the accelerator structure after initially heating the filament assembly. Presumably this effect was minimized but not eliminated by the addition of the vacuum sealed accelerator door and vacuum pumping of the accelerator during the payload build up prior to launch.

The low altitude range of this flight imposed a severe test on the prototype electron accelerator design. The engineering design of the accelerator module to be utilized on the EXCEDE II experiment was successfully tested by the flight of PRECEDE II. The GEODSS video system tracked the accelerator tungsten filaments until payload impact.

3. ROCKETBORNE LN₂ COOLED INTERFEROMETER

Results of the engineering test of this instrument are described in Chapter 2 of this report.

4. GROUND BASED MEASUREMENTS: HOTEL SITE

The camera systems located at this site were deployed by TIC, Inc., and are described in Chapter 3 of this report.

5. GROUND BASED MEASUREMENTS: SE 70 SITE

A Photo Sonics cine sextant mobile tracking mount at the SE 70 optical site (see Figure 1-1) supported four optical systems as summarized in Table 1-3. This site was selected so that the electron beam as constrained along the geomagnetic field would be viewed from an end on aspect, that is, along the magnetic field, when the payload was at apogee assuming a nominal payload trajectory. The electron induced atmospheric emissions as viewed from this location present a minimal source size and thus a maximum exposure in the film recording camera and image intensified spectrographs at this site. In addition the small source size reduced the field of view required for the dual channel telephotometer and thus maximizes

the contrast ratio between the electron accelerator induced emissions and night sky radiations.

Table 1-3. SE 70 Site Ground Based Instrumentation

Instrument	Description	Purpose
AFGL Telephotometer	Dual channel photon counting telephotometer measures $N_2^+ 1N(0-0)$ 3914A and $O(^1S)$ 5577 A emissions.	Remote diagnostic of accelerator power output and records emissions of aeronomic interest.
HSS, Inc. UV Cygnus	Image intensified spectrograph records emissions in 3200 to 6000A wavelength range with 6A resolution.	Documents altitude dependent radiant intensities (N_2 Vegard Kaplan, N_2 second positive, N_2^+ first negative,).
HSS, Inc. Super Cygnus	Image intensified spectrograph records emissions in the 4200 to 7500A wavelength range with 1A resolution.	Documents altitude dependent radiant intensities (N_2^+ first negative, O_2^+ first negative, $O(^1S)$, N_2 first positive, N_2^+ Meinel, ... ²).
WSMR Camera	35 mm Cine camera, 264 cm focal length f/8 lens, operated at 6 frames per second.	High spatial resolution system documents accelerator performance, tracking mount performance and assists interpretation of spectrograph data.

The dual channel telephotometer located at the SE 70 site recorded the accelerator induced $N_2^+ 1N(0-0)$ band at 3914A as a remote diagnostic of accelerator performance and the $O(^1S)$ 5577A emission because of its aeronomic interest. Selected samples of the telephotometer data are presented in Figures 1-7 and 1-8. Note that the arcing mode of accelerator operation was documented by the ground based telephotometer indicating that, in this mode, some fraction of the energy drawn from the high voltage battery pack is deposited in the atmosphere. The $N_2^+ 1N(0-0)$ emission at 3914A monitors the total electron power deposited in the atmosphere as demonstrated in the initial PRECEDE launch (O'Neil et al, PRECEDE: Summarized Results, JGR, 1978).

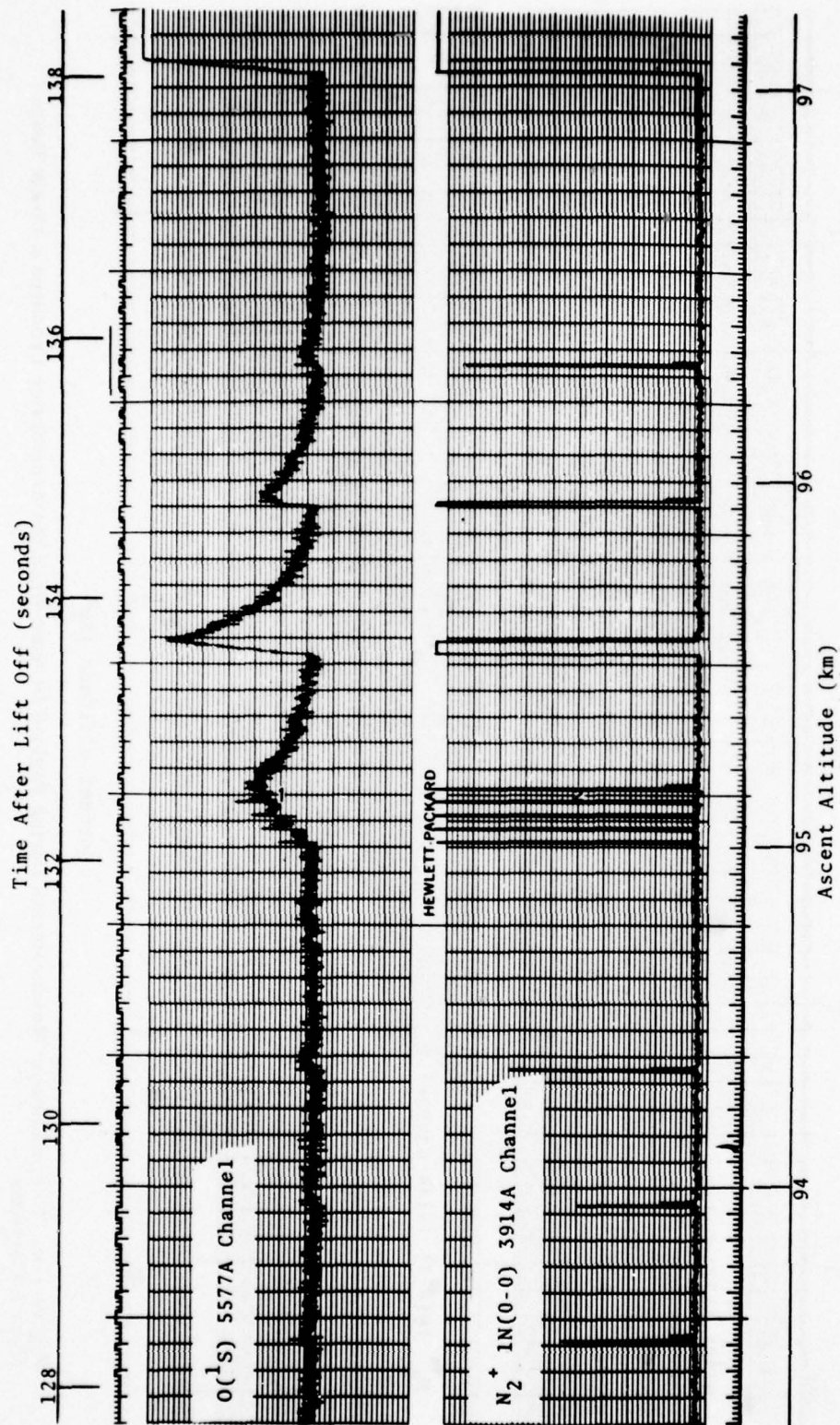


Figure 1-7. Sample of Telephotometer Measurements During the Initial Period of the Experiment

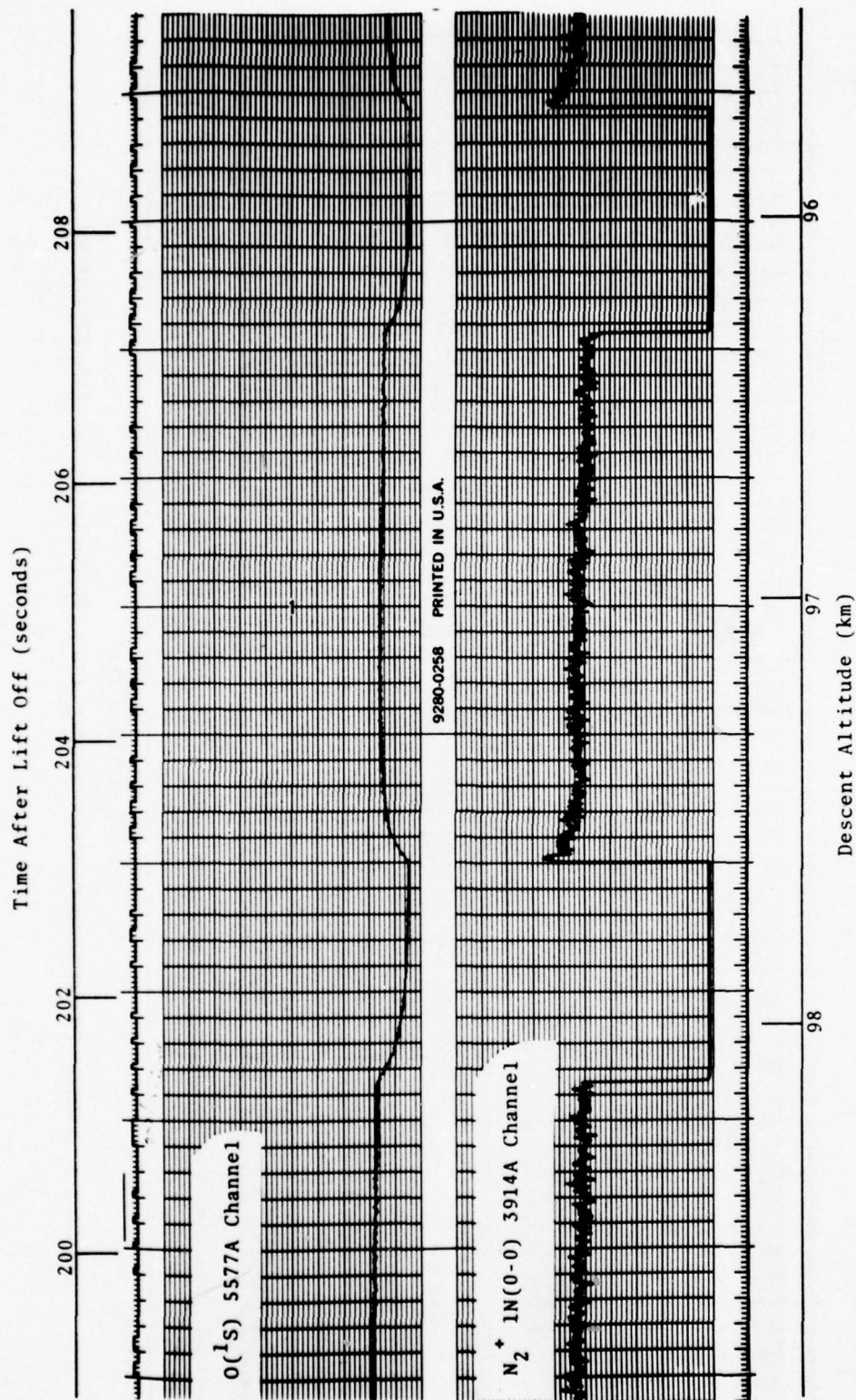


Figure 1-8. Telephotometer Measurements During Payload Descent When the Accelerator Produced a 15-kW Beam of 3 kV Electrons

The photometer measurements precisely monitor the absolute radiant intensity of the N_2^+ 3914A and $O(^1S)$ 5577A emissions. These measurements will eventually be correlated with the image intensified spectrographic measurements to determine altitude dependent emission profiles for a number of emissions in the 60 to 100 km altitude range. In particular, insight into the production and quenching coefficients for the N_2 first positive and N_2^+ Meinel bands are anticipated from the spectrographic measurements. The complicated altitude dependent production and loss mechanisms determined for the $O(^1S)$ 5577A emission in the initial PRECEDE launch will be tested against the newly acquired PRECEDE II data. The tele-photometer and spectrographs recorded accelerator induced emissions as low as 63 km in the present experiment, providing data at higher collision frequencies to test collisional deactivation rate coefficients inferred from the initial PRECEDE experiment.

A preliminary assessment of the results of the spectrographic measurements is given in Chapter 4 of this report.

6. GROUND BASED MEASUREMENTS: STALLION SITE

The satellite optical tracking station at the Stallion site (see Figure 1-1), developed and directed by the Electronics System Division of the Air Force Systems Command with contractor support from the Lincoln Laboratory of MIT, graciously agreed to attempt to manually track and record the accelerator induced optical emissions with their 14-in. and 31-in. diameter satellite tracking telescope systems. The common telescope mount was directed to the angular orientation where the initial accelerator pulse was anticipated assuming a nominal trajectory. The GEODSS facility readily observed the accelerator induced emissions in the wide angle (7-deg) 14-inch system, subsequently acquired the source in the narrow field (1.2-deg) 31-in. system and manually tracked the source (atmospheric emissions and/or hot filaments) until the minimal amount elevation limit (18 deg) was reached. Selected frames from the video recordings are shown in Figures 1-9, 1-10, and 1-11. Figure 1-9 occurred at a time shortly after electron accelerator pulse turn on and consists of prompt emission along the magnetic field with a small afterglow radiation, $O(^1S)$ 5577A emission, beginning to develop. Figure 1-10 shows a video image later in a 4.3 sec pulse and shows the spatial extent of a well developed $O(^1S)$ afterglow emission. Figure 1-11 illustrates the images of both newly initiated pulse and the long lived decay of the previous pulse terminated at least 1.7 earlier. As viewed from the Stallion Site the projected geomagnetic field at the payload location has an apparent elevation angle of approximately 45 degrees. The GEODSS data illustrates that the time dependent emission profile of relative slow optical emissions may be determined by

measuring the spatial extent of the afterglow radiation of these features. The GEODSS data will be further analyzed in terms of electron range along the magnetic field, image size, and afterglow emission profiles when the payload pitch angle orientation is determined.

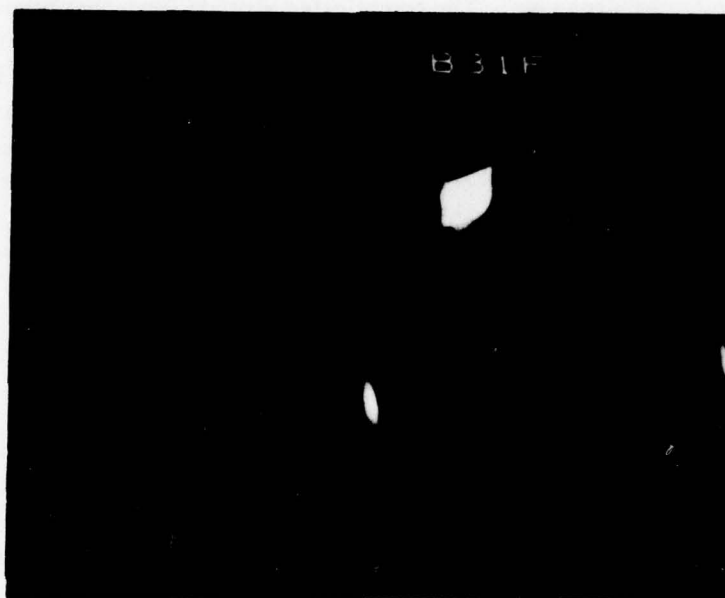


Figure 1-9. Image Recorded Shortly After Accelerator Pulse Initiation Showing a Very Slight Afterglow Emission

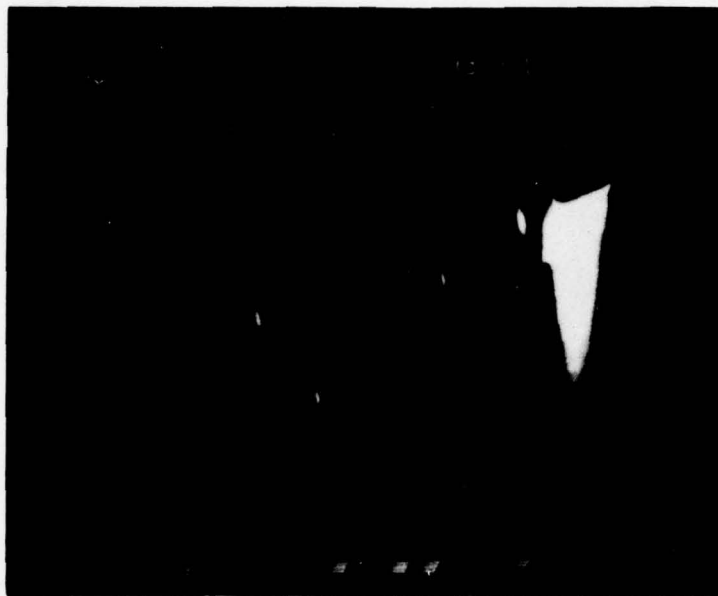


Figure 1-10. Image Recorded 140 sec After Launch During the Initial 20 kW Electron Accelerator Pulse at 98 km on Payload Ascent (GEODSS facility)



Figure 1-11. Image Recorded 154 sec After Launch, Payload at an Ascent Altitude of 101 km (GEODSS facility)

2. Rocketborne LN₂ SWIR Interferometer

J.C. Kemp and R.J. Huppi
Stewart Radiance Laboratory
Bedford, Massachusetts 01730

1. INSTRUMENTATION DESCRIPTION

The Michelson interferometer is dependent upon a moving mirror to change the relative optical pathlength of the two interfering beams of light. The mirrors must be carefully aligned to maintain proper coincidence of the two beams. Therefore, strict requirements are placed upon the translation accuracy of the moving mirror; the mirror direction must be maintained constant to within about 1 sec of arc throughout the useful scan range.

A system to allow mirror translation movement without angular movement has been designed using Bendix free-flex flexural pivots. A pictorial schematic showing the main elements of the interferometer assembly is shown in Figure 2-1. The mirror translation is driven by a torque motor. A linear variable differential transformer provides position feedback and a tachometer similar to the torque motor provides velocity feedback to the mirror translation servo. The second mirror of the Michelson system remains fixed in position. This stationary mirror is mounted to an assembly of three piezoelectric stacks, which provide fine adjustments of mirror orientation to optically align the interferometer. The beamsplitter and compensator are made of calcium fluoride.

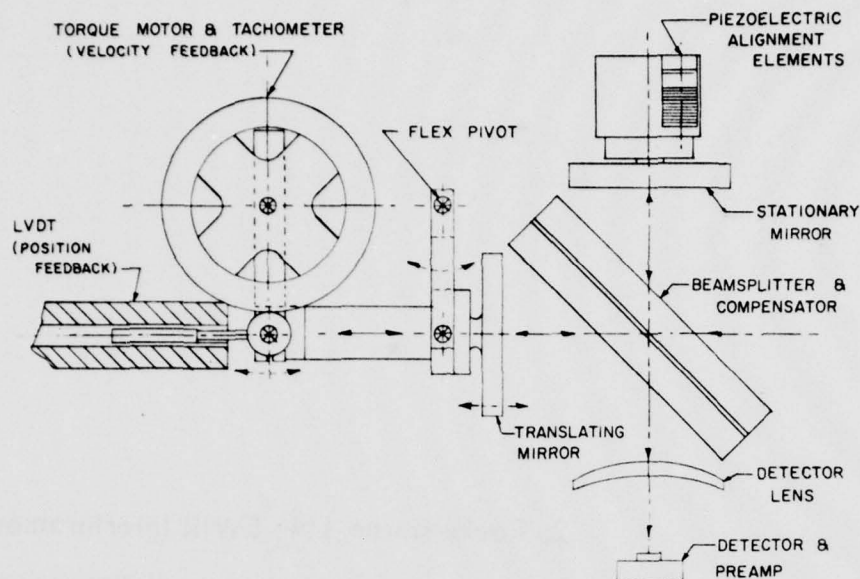


Figure 2-1. Schematic of Interferometer Assembly

A reference interferometer assembly is used to provide information about the center of the interferogram and also to provide main channel sampling data. The same mirrors and beamsplitter are used for the reference and the main channels by using some of the peripheral area of the elements of the main channel and feeding these signals in reverse direction through the interferometer assembly. The reference sources are located near the main channel detector and the reference detectors are located near the main channel entrance aperture. An incandescent bulb is the source of the whitelight channel, which defines the center position indication (zero path difference for the fixed and movable mirrors). The sampling reference is provided by the monochromatic reference channel using a neon glow lamp as a source. A narrow band optical filter is required to isolate a single emission line of the neon spectra.

Indium antimonide at liquid nitrogen temperature (77°K) is used for the main channel detector. A D^* improvement of about 2 orders of magnitude is achieved by also cooling the background to which the detector is exposed. Thus a 2 order of magnitude improvement in NESR is achieved by cooling the entire interferometer to liquid nitrogen temperature. This is very significant because the measurement time is reduced by 10^4 if the same signal to noise is maintained. The instrument is cooled by building it into a cryogenic Dewar which is a vessel with a reservoir for

the cryogen (liquid nitrogen) and a region for the instrument to be cooled, all located inside of a vacuum shield to act as a thermal barrier. Once the Dewar is lofted to the required altitude by the rocket carrier, the Dewar is opened to expose the optics to the radiation to be measured.

A special preamp is required by the high sensitivity of the InSb detector under cold background conditions. A dual source follower FET attached directly to the detector mount drives the preamp output stage located in the warm aft section of the Dewar. This stage drives a balanced line feeding a differential input instrumentation amplifier located in an external electronics box. All of the circuitry required for the main channel signal conditioning, reference interferometer signal conditioning, temperature monitors, and the mirror drive servo is located in the external electronics box. A separate battery box supplies isolated power to the various electronic circuits to help maintain a very low noise system.

The very high sensitivity of the system also means that the background radiation from the warm earth exceeds the minimum detectable signal. Therefore a cold sunshade baffle is required within the Dewar to provide high spatial rejection for off-axis sources. This baffle will provide more than 8 orders of magnitude reduction in the signal level from sources located more than 50° away from the system axis. The design specifications for the rocketborne LN₂ interferometer are summarized in Table 2-1.

Table 2-1. Design Specifications for the LN₂ Cooled Michelson Interferometer

Spectral Range	2.0 - 5.6 μ
Resolution	2 cm ⁻¹ (apodized)
Field-of-View	2.29°; 1.26×10^{-2} sr
Collection Optics Area	17.8 cm ²
Scan Time (variable)	2.0 sec total 0.2 sec retrace 1.8 scan period
NESR*	7×10^{-11} W/cm ⁻² sr ⁻¹ cm
Size	10.5 in. diam \times 29.3 in. long (+ electronics)
Weight	54 lbs (+ electronics)

*Noise Equivalent Spectral Radiance at 2 μ

2. EXPERIMENTAL APPROACH

PRECEDE II provided an engineering test of a newly developed rocketborne LN_2 interferometer in an operating environment simulating the follow on EXCEDE II experiment. As proposed, PRECEDE II was designed to test the engineering design of the LN_2 interferometer operating onboard a payload also containing a prototype 20-kW pulsed electron accelerator. These two newly developed rocketborne instruments, the interferometer using cold optics and the high power accelerator module, are the innovative systems developed for the EXCEDE II experiment. PRECEDE II was intended to test each instrument independently in a realistic rocket environment as well as the compatibility of the instruments sharing a common payload structure. No attempt was made to co-align the electron beam and the interferometer viewing axis. Preflight estimates indicated the interferometer would probably not record the electron beam induced infrared emissions given the payload configuration for this engineering test flight.

3. LN_2 INTERFEROMETER SUMMARIZED RESULTS

The engineering test demonstrated that the cooled Michelson interferometer design is well suited for taking data in a rocket environment. All of the system components functioned well for the entire flight. The cryogenic system, the batteries, the detector and drive electronics, the temperature monitors, and the battery status indicators performed according to design. An inflight calibration source provided a useful indication of the interferometer internal optical alignment. The piezo electric mirror adjustment system proved to be an effective method of performing final optical alignment of the interferometer, even at cryogenic temperatures.

It was demonstrated that proper interferometer internal optical alignment can be achieved after the interferometer has been mounted to the payload, that the payload can be mated to the motors, and that the entire assembly can be transported to the launch area and erected in the tower without any major alignment problems. It was also determined that because of the shocks received during these processes it is necessary to perform final internal alignment after the payload is erected in the tower.

The interferometer's internal optical alignment deteriorated somewhat during the launch cycle. The modulation efficiency just prior to launch was about 44 percent; after launch the alignment had changed sufficiently to reduce the modulation efficiency to about 7 percent. Although 7 percent is less than desirable, good data would still be achieved during the EXCEDE 78 launch if the signal emission levels are as large as predicted.

Some results from the engineering test are shown in Figures 2-2 through 2-5. Because of the non-optimum monochromatic reference the interferometer resolution is degraded below the designed 2 cm^{-1} . Also, for this flight, the interferometer was operating in a double sided interferogram mode rather than the single sided mode which will be used in the actual data flight.

Figure 2-2 shows the strip chart of the FM/FM transmitted interferogram recorded 288 sec into the flight. This late in the flight the payload was coning badly. The bottom trace of this figure is a recording of the monochromatic reference channel; the decreased width indicated the retrace portion of the scan. Figure 2-3 shows the spectrum transformed at USU from this interferogram. The spectral features probably result from atmospheric thermal emissions.

Figure 2-4a shows the spectrum obtained from the internal calibration source before launch and Figure 2-4b shows the spectrum from the same source 72 sec after launch. The loss in internal alignment is very apparent at the shorter wavelengths but the longer wavelengths show no appreciable change. These spectra allow us to infer that the misalignment was on the order of 4 arc sec or less.

Figure 2-5 shows a spectrum transformed from data taken 187 sec into launch which corresponds to a time when the gun was firing. The emissions apparent in the spectrum are primarily due to ambient atmospheric thermal radiation.

4. FUTURE EFFORT

The major effort in preparation for the EXCEDE 78 launch will be the development of an improved monochromatic reference. The reference electrical circuits need to be improved somewhat but the most important need is for a much stronger source of monochromatic radiation. It will probably be necessary to use a HeNe laser mounted outside the Dewar for this source and to use an optical fiber to transmit the optical energy into the Dewar to the reference interferometer. The previous reference system used a neon light with a narrow band optical filter as the source of monochromatic radiation.

Two other areas of focus are to improve the rigidity of the internal alignment to eliminate the degradation in modulation efficiency which occurred during the launch. More extensive shock and vibration tests will be conducted in an attempt to verify that the stability has been improved.

Operational techniques also need to be refined to expedite final alignment adjustment at the launch pad. Also the clean payload conditions required by the additional helium cooled spectrometer on the EXCEDE 78 payload necessitate a modification in the Dewar to prevent possible escape of any trapped dust particles. Other minor electronic circuit improvements will be made.

A complete calibration and performance verification will be performed.

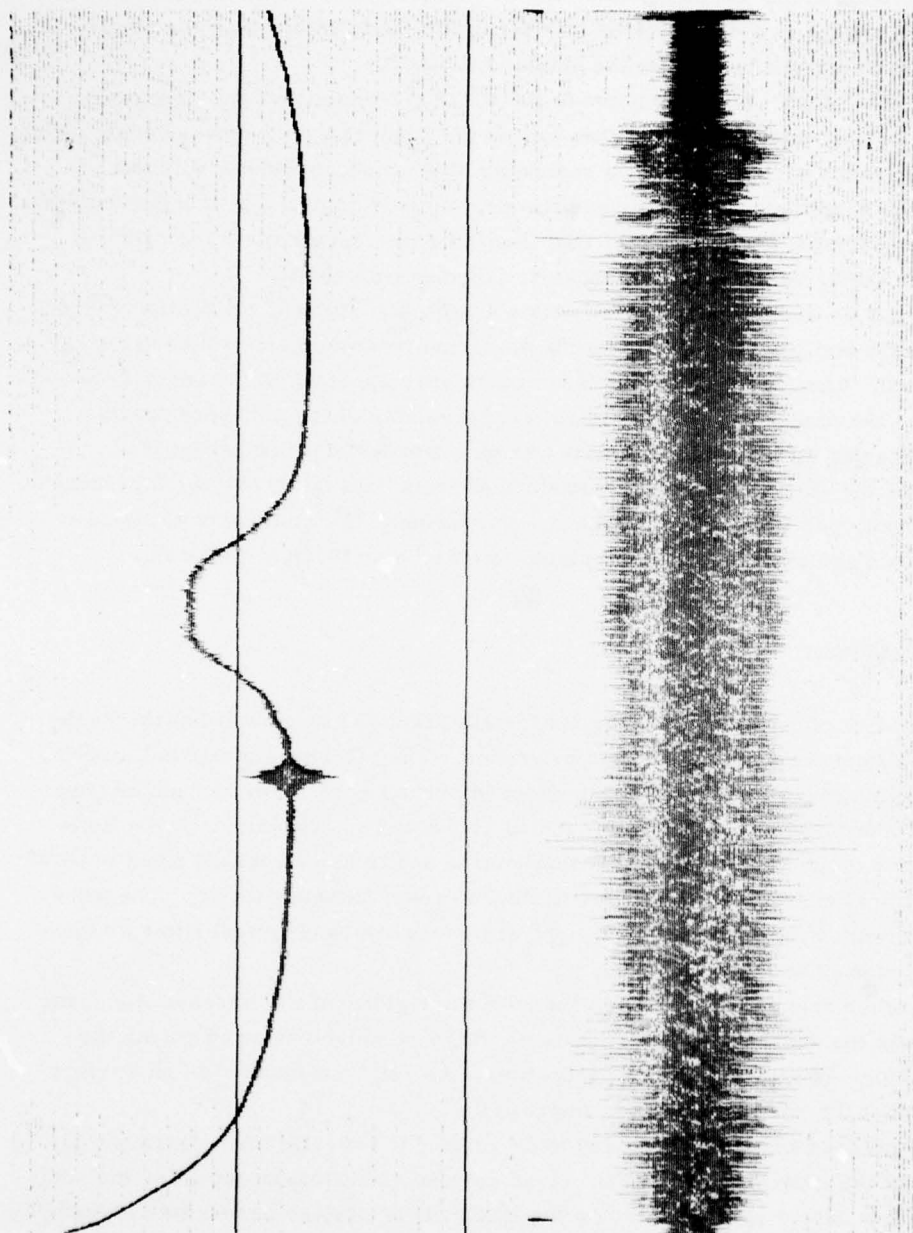


Figure 2-2. Interferogram Recorded at T+238 sec and Monochromatic Reference

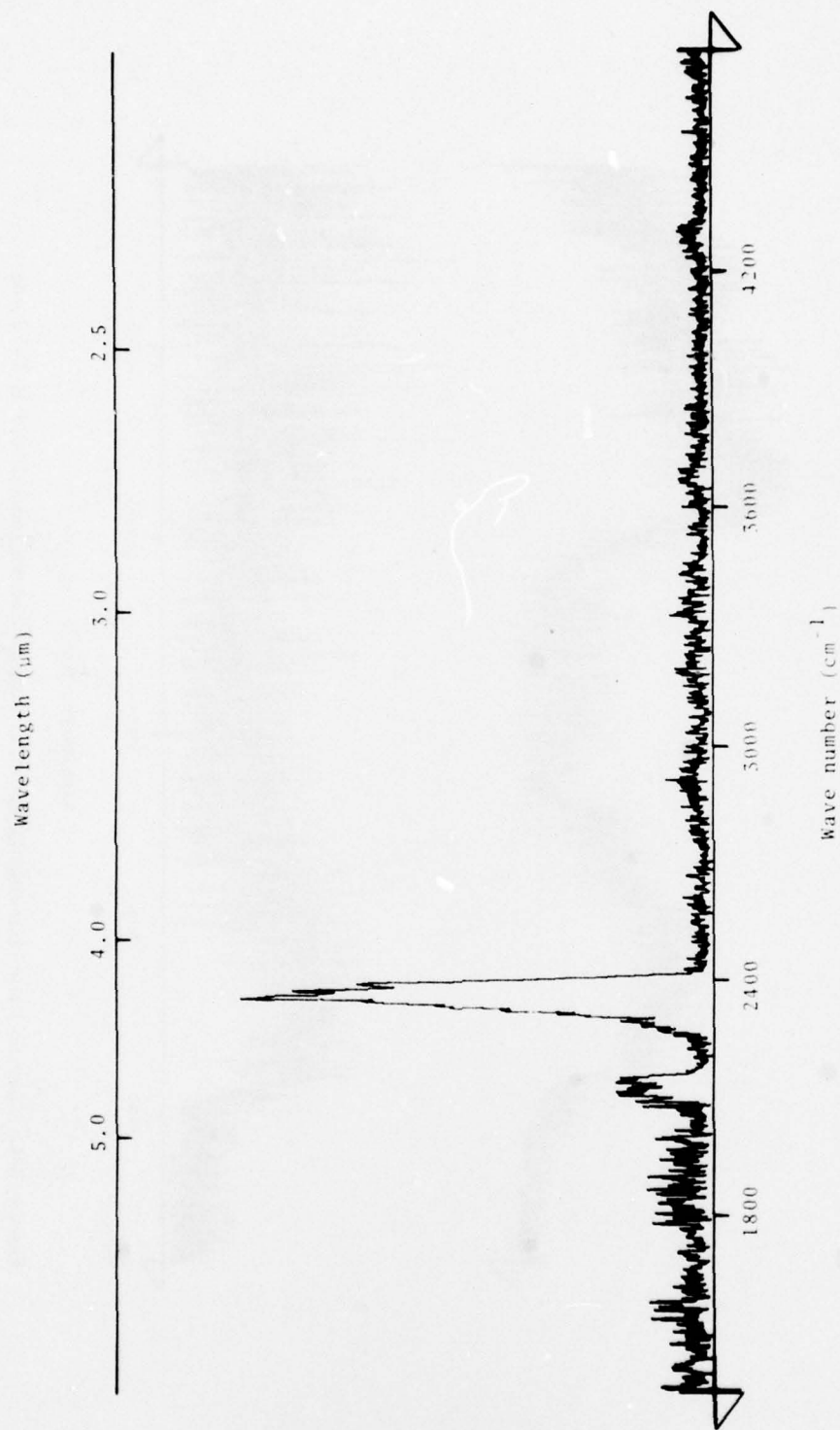


Figure 2-3. Spectrum Transformed From Interferogram Taken at T+288 sec

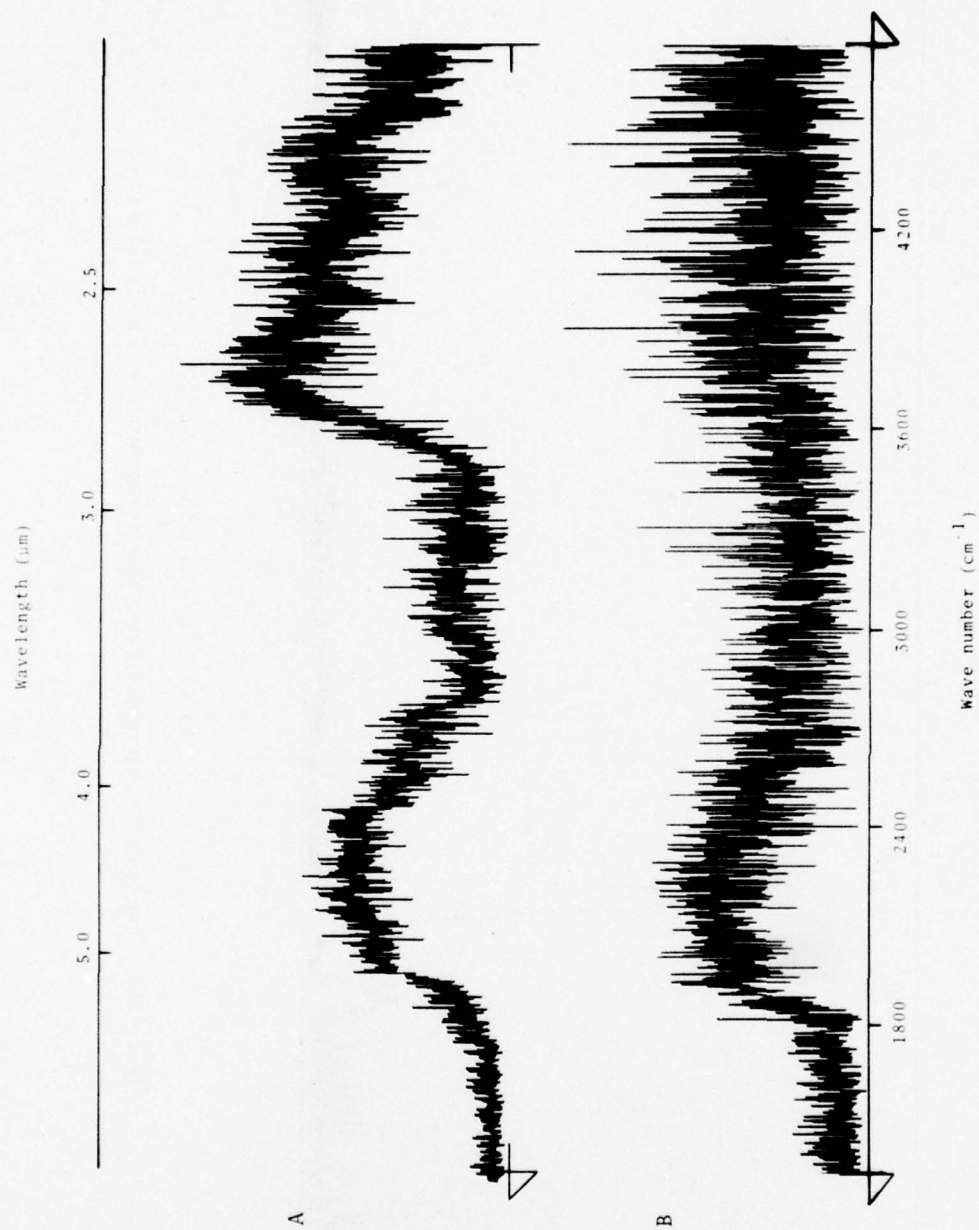


Figure 2-4. Spectra From Internal Calibration Source Before Launch and at T+72 sec

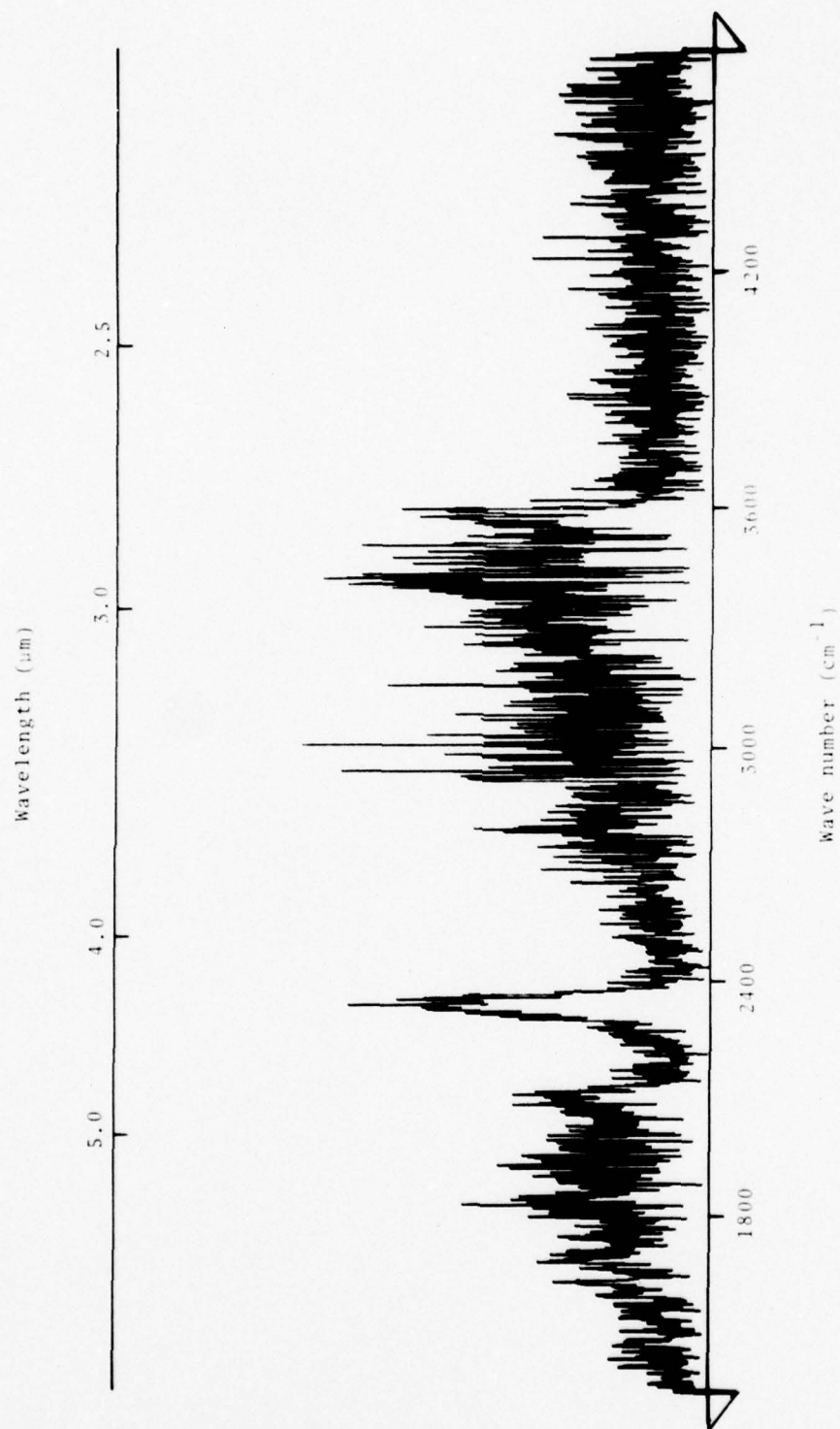


Figure 2-5. Spectrum From T+187 sec

3. Hotel Site Ground Based Optical Measurements

W. Boquist and R.W. Deuel
Technology International Corporation
Bedford, Massachusetts 01730

1. INTRODUCTION

This quick-look chapter summarizes the operational results of photographic measurements made by Technology International Corporation in participation with the Optical Physics Group of AFGL during the Project PRECEDE II exercise conducted at White Sands Missile Range, New Mexico, on 12 December 1977. The purpose of TIC's participation was to provide high resolution photographic coverage of the optical effects of the PRECEDE II electron gun experiment at altitudes of between 90 and 120 km. More specifically, acquisition of temporal spatial and radiometric data of the visible field aligned beam and slower decaying induced afterglow was desired in order to correlate the overall performance of the rocket borne experiment and provide data for the study of upper atmospheric excitation characteristics. This approach was predicated on the successful coverage provided by TIC on the previous PRECEDE experiment, also conducted at WSMR by AFGL, in the fall of 1974.

TIC's participation was limited to the operation of existing optical instrumentation which could be fielded on the basis of operational costs alone. On this basis, TIC fielded a group of selected large aperture cameras and a low light level video system that were mounted on a radar guided tracking mount provided by the WSMR range complex.

The TIC instrumentation was located geographically such that it would view the field aligned visible beam from a perspective perpendicular to the geomagnetic field lines. This site would thus be able to acquire data which could be complementary to that obtained at the other AFGL site which was viewing the beam essentially along the field lines.

2. OPERATIONAL PROCEDURE

The AFGL PRECEDE II electron gun instrument package consisted of an electron beam accelerator which was planned to be activated above about 90 km continuing through apogee of about 120 km, and down to the vicinity of about 80 km in an on-off pulse cycle of approximately 4 sec (on) and 2 sec (off). Depending upon rocket de-spin results, the beam would either be directed in one (only) or two (both) directions along the magnetic field lines in proximity to the vehicle during the on portion of the duty cycle. The collisional excitation of the ambient upper atmosphere by the electron beam is the subject of optical interest and the spatial and radiometric recording of the directional beam above 90 km together with the chemiluminescent wake was the objective of the TIC optical instrumentation coverage.

The TIC optical instrumentation was located at the Hotel site on the southeastern edge of the White Sands Missile Range so as to be looking essentially due west when the PRECEDE II payload was at apogee (see Figure 3-1). The Air-Land Division of Dynaelectron Corporation provided technical support to the Hotel optics site by way of a radar controlled tracking mount for the primary optical instrumentation. This mount was a Photo-Sonics Cine-Sextant Mobile Tracking Mount operated by a crew of two.

Both tracking and fixed camera systems were operated by TIC in support of the AFGL PRECEDE II experiment. The primary camera system consisted of a large aperture 300-mm focal length lens and film transport. Operated simultaneously with this camera was a second 300-mm system of smaller aperture which incorporated a clock for determining exposure time and duration. In addition, a wide field-of-view time lapse camera system was operated independently to record the flight and provide a projection print, if required, for subsequent analysis. All three of these camera systems were co-located on the mobile tracking mount, together with a low light level TV system to aid the camera control operator in transporting the film of the shutterless cameras during the off portion of the electron gun duty cycle.

As a limited back-up to the primary tracking instrumentation, 2 fixed, ballistic mode cameras were operated at the Hotel site by TIC. This concept, although previously untried in these experiments so far as is known, was implemented to provide an optical record of payload brightness and pulse duration as a function of altitude on a single film frame. Table 3-1 summarizes the TIC optical instrument plan for PRECEDE II, showing for each system the collector characteristics, film type, exposure program, and recorded field-of-view.

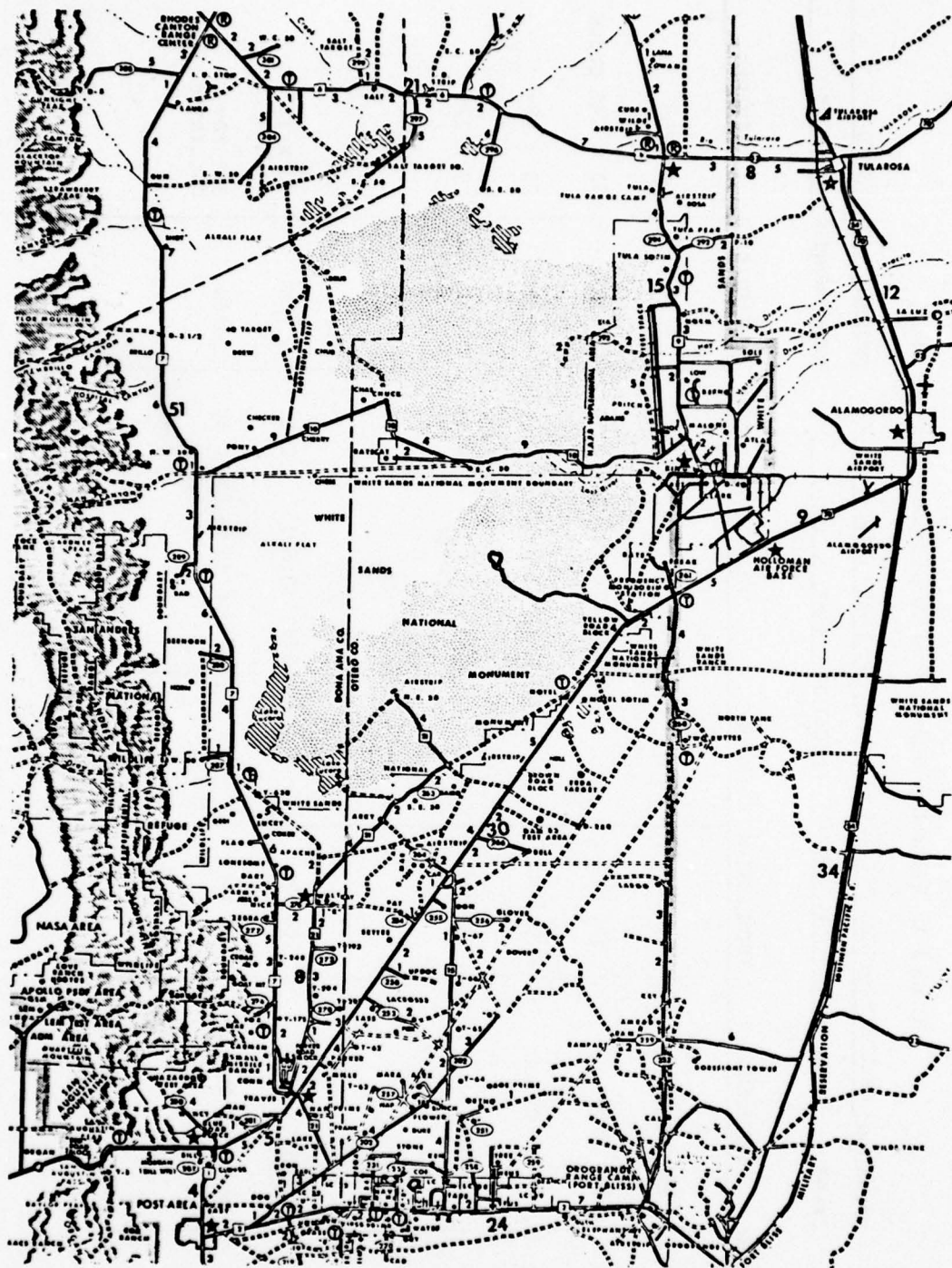


Figure 3-1. White Sands Missile Range Map

Table 3-1. Technology International Corporation Instrument Plan

OPERATION: EXCEDE PROGRAM: PRECEDE II DATE: 12 DECEMBER 1977 STATION: HOTEL SITE
 EVENT: 3 KV 20 KW ACCEL. TEST LOCATION: WSMR, N.MEX. PROJ./ENGINEER: AFGL/OPR

POSITION	INSTRUMENT	FOCAL LENGTH	FILTER	FILM	f/r	SHUTTER/RATE	REMARKS
01	300 DELFT	300 MM	-	2484 70 X 15'	0.90	4 SEC	10° FOV
02	300 KODAK	300 MM	-	2484 70 X 100'	2.5	4 SEC	11 X 14° CLOCK
03	FR IV C	50 MM	-	2484 35 X 100'	0.95	2 SEC	21 X 28°
04	COHU 4400	50 MM	-	VIDEO 1/2" X 2400'	0.95	1/30 SEC	9 X 12°
11	EL-500	100 MM	-	2484 70 X 15'	2.0	OPEN	32 X 32° FOV BALLISTIC
12	H-8/FARRON	76 MM	-	EP-200 70 X 15'	0.87	OPEN	30° FOV BALLISTIC

The Hotel optical site was supported by the DNA photo-optical van operated by TIC. The van contains a darkroom for loading film and processing test focus runs, an analysis room for reviewing processed film, and an operation section which houses the camera control electronics, recorders, timers, and power supplies.

A live test of all primary and secondary camera systems was made on 10 December 1977 on a non-related rocket experiment which attained a comparable apogee and location after dark. All camera systems operated properly during this test, but in processing the data it was observed that the mobile tracking mount was unable to track smoothly when in the extreme elevated position. As a consequence of this determination, the Hotel site mount was changed prior to the PRECEDE II launch. No testing of this mount was possible, however, before the PRECEDE II launch.

3. RESULTS

3.1 Weather

The weather at event time (10:52 Local Time) can be described as generally clear at low altitudes with readily noticeable atmospheric motion apparent overhead as seen from the Hotel optics site.

3.2 Event Data

The PRECEDE II event was launched at 05 49 59.1 UT from the launch complex LC-36 on 13 December 1977. An apogee of 102 km was reached at 171 sec after launch. The electron gun began its function mode at approximately 138 sec at 97 km altitude and continued to operate until it had descended to 74 km altitude at approximately 249 seconds.

3.3 Instrumentation Performance

The high resolution photographic instrumentation performed well throughout the experiment. No malfunctions were evident. Focus changes due to ambient temperature changes were essentially corrected for, although with notable difficulty. (The photographic quartz data chronometer, also affected by cold temperature, was 2 sec slow in 2 days by event time.) The time lapse camera system worked well with an occasional double film frame transport, probably due to a slightly longer than optimum trigger pulse.

Use of a low light level TV system to inform the camera control operator when the electron gun was off (in order to advance the film shutterless cameras without dragging the image) worked extremely well. An additional TV monitor located outside the control trailer was found to be of significant value in informing the

secondary mount operator and others as to the general track centering, etc. Attempts to record the video signal, however, were generally negated by the lack of frequency stable power at the Hotel site, which was powered by a portable gasoline generator.

The secondary (priority) ballistic camera attempt was conceptually a definite success, although the shutter(s) could have been opened earlier to have captured a longer ballistic track than was obtained.

The performance of the cine-sextant tracking mount was found to be generally unsmooth when operated at elevation angles above about 60°. As a consequence, the typical 4-sec exposures were often too long (as evidenced by star tracks) to produce a steady track segment. Since this condition exists in apparently all mounts of this manufacture, the site should have, in retrospect, been further east so that a 60° elevation angle would not have been exceeded in performing the missile track.

3.4 Photographic Data

All of the data records from the Hotel optics site obtained photographic images of the event with the exception of the video system recorder. However, inasmuch as the rocket payload did not exceed 102 km in altitude, the visible electron induced beam image due to the prompt N_2^+ emissions as well as the longer lived $O(^1S)$ emissions was limited to the order of a kilometer or less in length and was to a large degree integrated into a single image with the exposure times used in anticipation of a 120-km apogee trajectory. Examination of the images contained in the primary data record tend to show the following: a small nearly circular image with a growing tail as the rocket ascends in altitude. During this period, the mount tracked relatively smoothly, as evidenced by the star track images. At higher altitudes the source image shows what appears to be two partially overlapping images. At these mount elevations, however, some of the star tracks indicate significant hunting in the mount motion and some of these images will probably not be valid.

Over 35 frames of data were obtained by the primary camera system. Table 3-2 correlates the record frame number with exposure (end) time and vehicle altitude from launch through reentry. Table 3-3 correlates the electron gun duty cycle with time after launch for comparison with Table 3-2.

Table 3-2. TIC Photographic Record 40401
(Preliminary)

Frame No.	Time UT	Exposure Length	Time After Launch	Vehicle Altitude
--	05 49 59.1 hms	-- sec	0 sec	1.2 km (Launch)
1	51 39	--	100	78
2	52	13	113	86
3	54	2	115	87
4	52 00	6	121	90
5	06	6	127	93
6	02 52 10 hms	4 sec	131	94.5 km
7	20	10	141	98
8	27	7	148	100
9	32	5	153	101
10	39	7	160	102
11	05 52 45 hms	6 sec	166 sec	102 km
12	50	5	171	102 (Apogee)
13	57	7	178	102
14	53 02	5	183	102
15	09	7	190	101
16	05 53 15 hms	6 sec	196 sec	99.5 km
17	20	5	201	98
18				
19	32			
20	38	6	219	92
21	05 53 44 hms	6 sec	225 sec	89 km
22	50	6	231	86
23	55	5	236	83
24	54 00	5	241	79
25	07	7	248	75
26	05 54 13 hms	6 sec	254 sec	70 km
27	20	7	261	64
28	24	4	265	61
29	29	5	270	56
30	34	5	275	52 (begin tumbling)
31	05 54 40 hms	6 sec	281 sec	46 km
32	45	5	286	40
33	50	5	291	35 (6 images)
34	56	6	297	29.5
35	55 00	4	301	26

Table 3-3. Electron Gun Duty Schedule
(Preliminary)

No.	Beam On	Beam Off	Pulse Duration
1	138.3 sec	142.3 sec	4.0 sec
2	144	145	1
3	146	148.3	2.3
4	149.9	150.6	0.7
5	151.7	152.8	1.1
6	153.8 sec	154.1 sec	0.3 sec
7	155.8	160	4.2
8	161.7	165.8	4.1
9	167.6	171.8	4.3
10	173.6	177.8	4.2
11	179.3 sec	183.7 sec	4.4 sec
12	185.3	189.7	4.4
13	191.3	195.6	4.1
14	197.2	201.4	4.2
15	203.3	207.5	4.2
16	209.1 sec	213.2 sec	4.1 sec
17	214.9	217.6	2.5
18	218.7	219.2	0.5
19	220.8	225.1	4.3
20	266.7	230.9	4.2
21	232.7 sec	237 sec	4.3 sec
22	241.6	242.8	1.2
23	244.4	248.8	4.4

Selected data frames of the accelerator induced emissions are presented in Figure 3-2, 3-3, and 3-4 for frames 8, 12, and 20 respectively. These photographs are a 15X magnification of the original data record, and show the electron emissions in ascent at 148 sec at 100 km altitude (frame 8), at 171 sec at apogee at 102 km altitude (frame 12), and at 219 sec at 92 km while descending (frame 20). Figure 3-5 shows the multiple visible filament images resulting from the tumbling of the reentering payload at 291 sec at 35 km altitude.

Figure 3-6 shows a portion of the PRECEDE II ballistic trajectory image as seen from the Hotel site perspective. The two visible portions of the payload trajectory correspond to electron gun cycles 20 and 21 as identified in Table 3-3 based upon preliminary timing determinations.

All photographic records except the ballistic data were processed with calibrated sensitometric control so that absolute image brightness determinations could be made in later analysis. The Kodak 2484 pan photographic data films were processed normally in D-19 developer to achieve a nominal gamma of 1 on the density log exposure plot of film sensitivity.

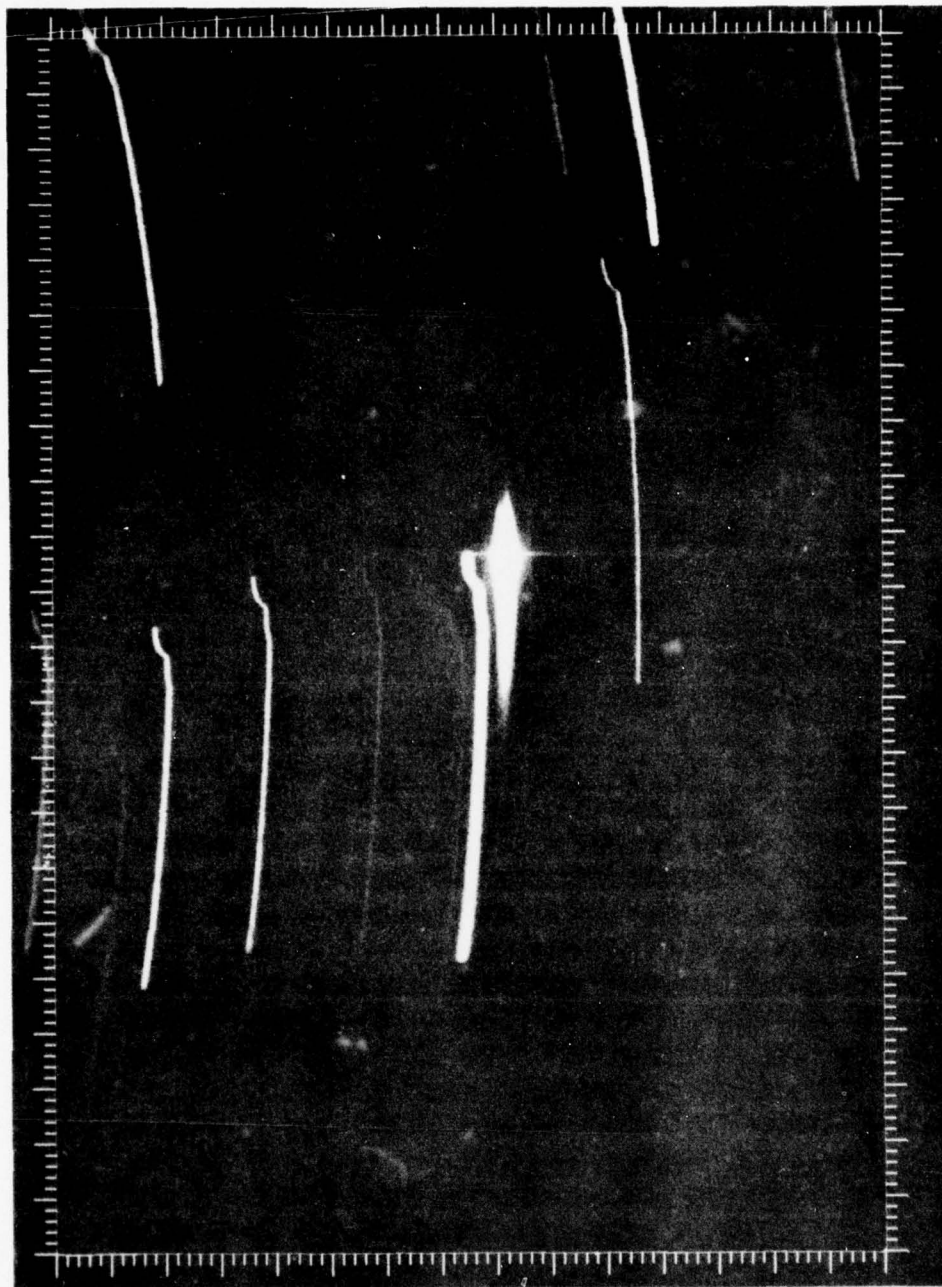


Figure 3-2. Image Recorded 148 sec After Launch, Payload at 100 km During Ascent

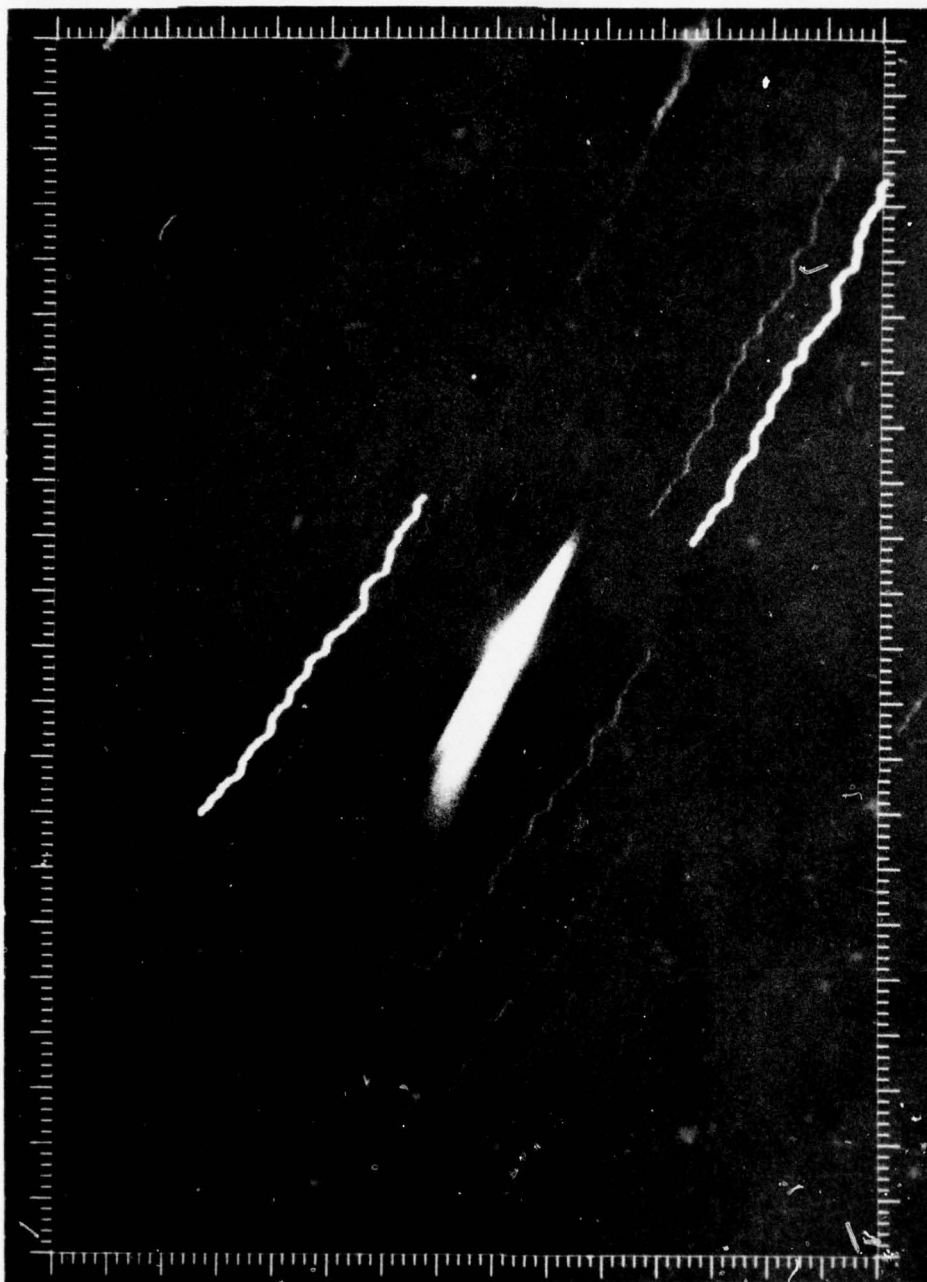


Figure 3-3. Image Recorded 171 sec After Launch, Payload at 102 km (apogee)

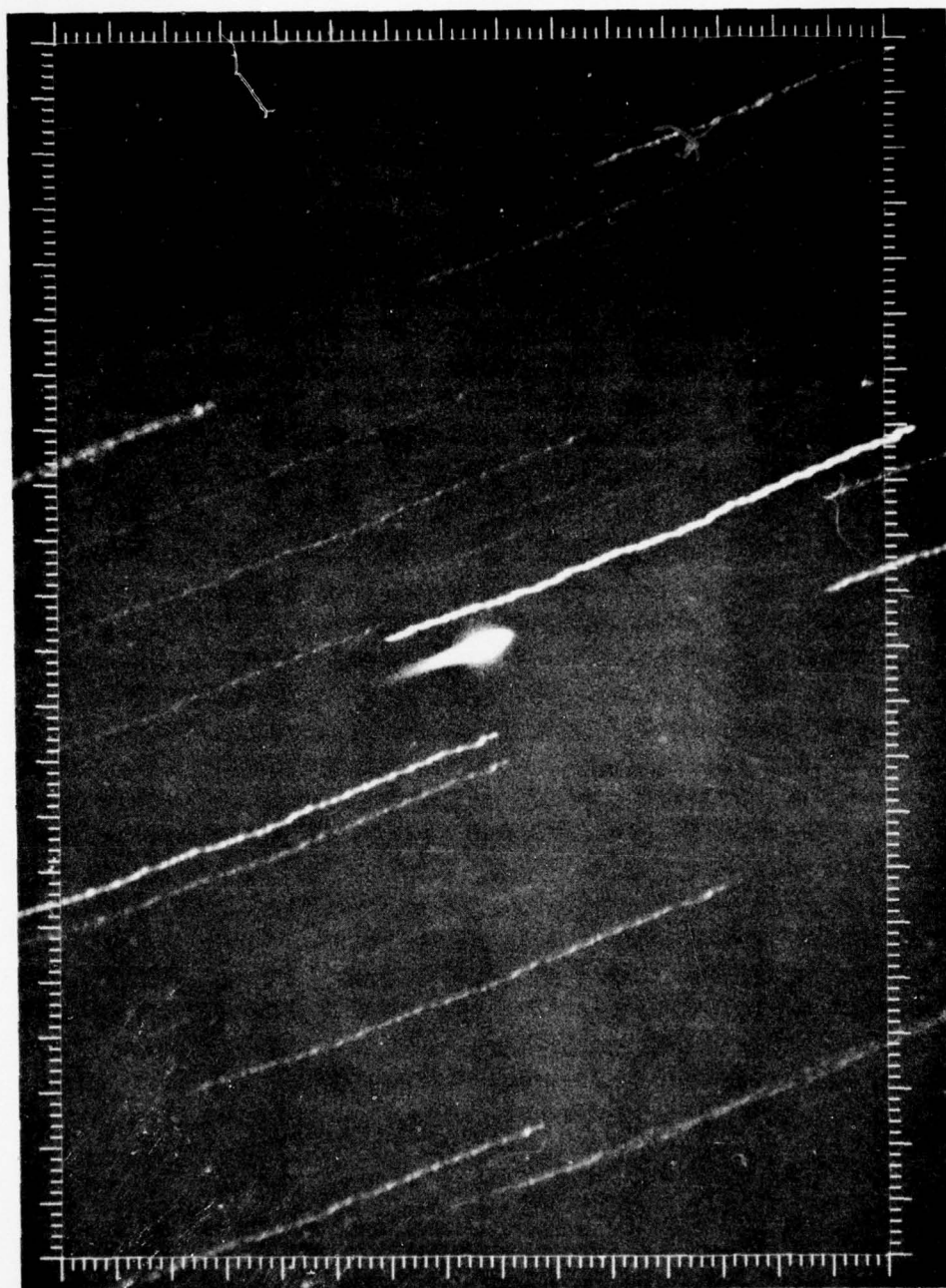


Figure 3-4. Image Recorded 219 sec After Launch Payload at 92 km on Descent

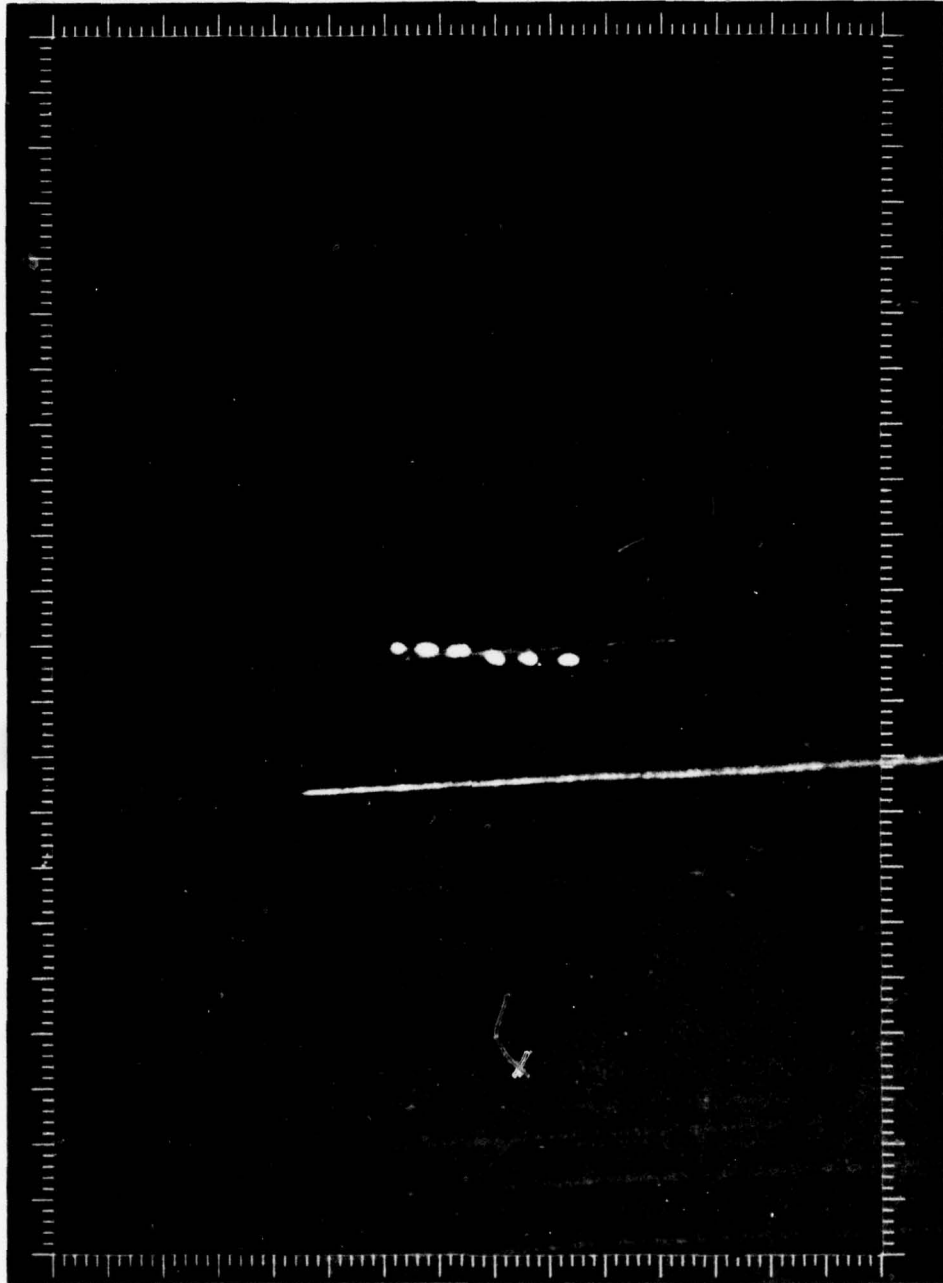


Figure 3-5. Image Recorded 281 sec After Launch, Payload at 35 km on Descent. Multiple images of the accelerator filaments recorded by the camera which no longer automatically tracked the accelerator at this point in the trajectory

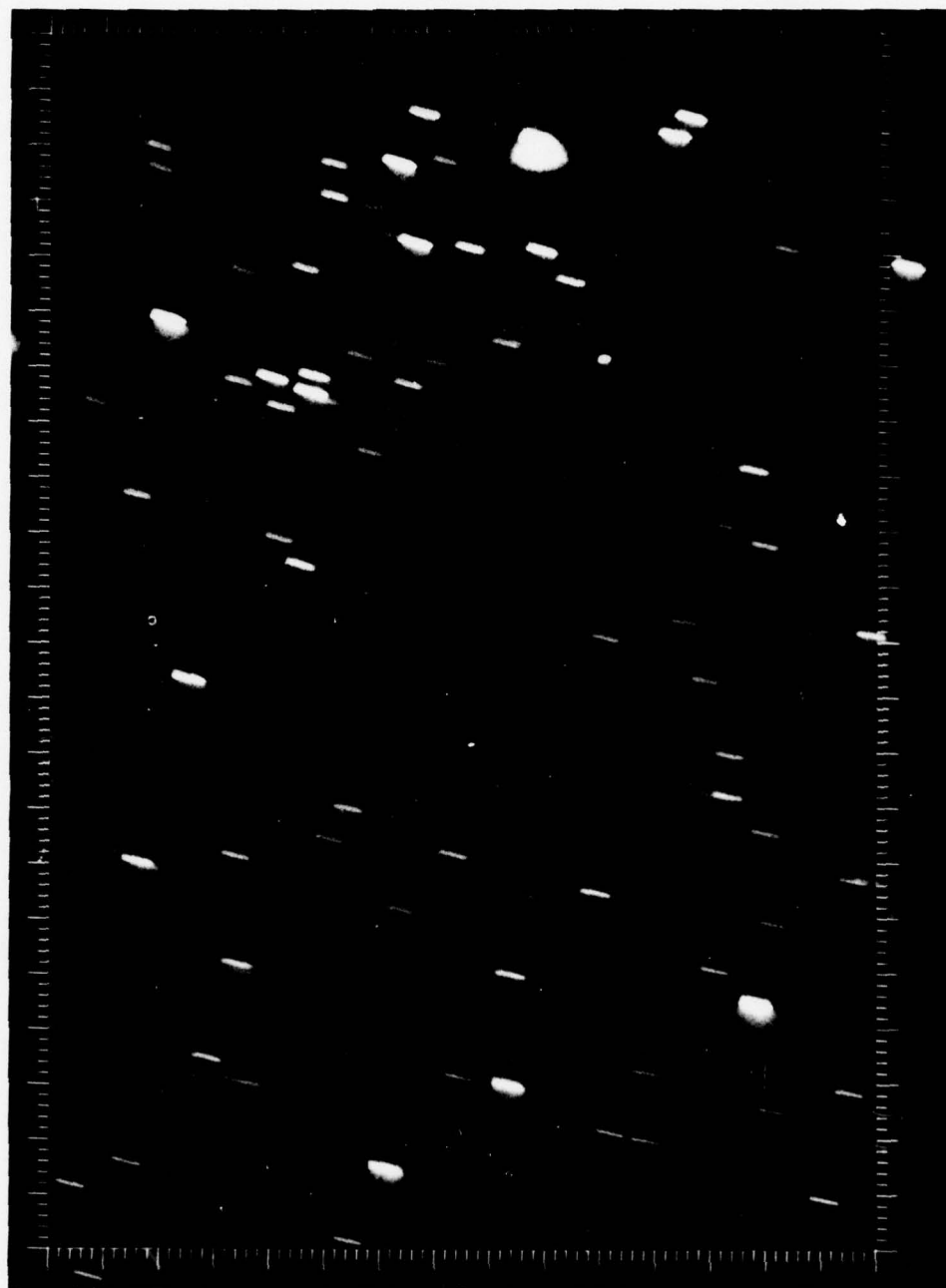


Figure 3-6. PRECEDE II Image Recorded by a Fixed Camera

4. CONCLUSIONS AND RECOMMENDATIONS

4.1 Instrumentation

Based upon PRECEDE II data results, it is clear that while certain instrumentation should be optimized for maximum lens-film sensitivity, other instrumentation should strive to minimize exposure time to negate any effect of irregular tracking mount motion when encountered. Moreover, a filtering of the prompt N_2^+ emissions with respect to the longer lived $O(^1S)$ emissions would be appropriate to consider for longer exposures. In general the selection of instrumentation systems used was appropriate for the objectives intended in PRECEDE II.

The ballistic mode cameras, having proven successful, should be expanded by using a complement of wider angle cameras (to 50°) and more sensitive lens cameras ($f/0.75$ at 150 mm) with, in at least one instance, a transmission grating to disperse the image spectrally in a direction perpendicular to the payload motion (at apogee).

In addition to the above, it would be especially useful to assure that sufficiently stable line power was available to permit video recording of the event for immediate review and to aid data processing decisions.

4.2 Mounts

The advantages in using a tracking mount are abundantly clear. This kind of mount should be used for appropriate instrumentation, when available. Other approaches to the tracking problem might include using an az/el mount positioned in the rocket trajectory plan so that only elevation would change, or using a three axis mount such that the azimuth motion could be aligned with the apparent payload motion for limited segments of acquisition time. In addition, however, a minimum complement of non-tracking (but trainable) camera systems should be incorporated in the optical plan for contingency utilization.

4.3 Site Location

As a consequence of experiences in PRECEDE II, it would be recommended that, relative to potential inherent tracking mount instabilities at high elevation angles and, in general, to optimize tracking perspective, a side viewing site be positioned further from the trajectory plane at a distance of 0.5 to 1.0 apogee which, for the former consideration, would obtain $60^\circ - 45^\circ$ maximum elevation angles.

4. SE 70 Site Ground Based Spectrographic Measurements

D.F. Hansen, M.P. Shuler, and L.B. Woolaver
HSS Inc.
Bedford, Massachusetts 01730

1. INTRODUCTION

This chapter provides quick-look information derived from image-intensified spectrographic measurements performed by HSS Inc. on PRECEDE II Event at White Sands Missile Range (WSMR) on the night of 12 December 1977.

An Aerobee 170 vehicle system (with nozzle extension) was used to loft a 685-lb payload which included a 3-kV, 7-A electron accelerator to an intended altitude of 115 kilometers. The vehicle was launched from WSMR Launch Complex 36 on an azimuth angle of 357° . The projected flight profile for the mission is given in Table 4-1.

HSS Inc. personnel deployed two ground-based image-intensified spectrographs at Southeast 70 site located 66 miles north of the launch site. The instruments were mounted on a WSMR mobile tracking mount which was remotely aimed by the WSMR PAS tracking system. The direction of the apogee point from Southeast 70 site was slightly west of due south.

Co-located on the tracking mount with the HSS Inc. instruments was an AFGL two-channel telephotometer. Also on the mount was a long focal length telescopic camera operated by WSMR personnel.

Table 4-1. PRECEDE II Projected Flight Profile

Time After Launch (sec)	Altitude (km)	Event
49.5	34	Sustainer Burnout
54	40	Commence Closure of Engine Valves
74	62	Despin Vehicle and Payload
83	70	Eject Clamshell Nose Tip
106	89	Commence Electron Injection
180	115	Apogee
267	80	Separate Payload From Vehicle
340	---	Vehicle Impact
500	4.6	Deploy Recovery System
650	---	Payload Impact

2. INSTRUMENTATION

2.1 Super-Cygnus Spectrograph

The instrument named Super-Cygnus was developed for the EXCEDE program under the sponsorship of the DNA in the 3 years between the PRECEDE I and II Events. On PRECEDE I Event (17 October 1974) HSS Inc. had deployed an image-intensified spectrograph called Cygnus which also had been developed under the sponsorship of DNA with AFGL as the technical monitor.

The Cygnus instrument was a low-dispersion, low-resolution spectrograph (200 Å/mm dispersion, 8 Å resolution) covering the wavelength region from 4200 Å to 8000 Å. On PRECEDE I Event, the objectives of this instrument were: (1) to aid in diagnosing the payload accelerator performance, (2) to back-up the payload photometers in case of any malfunction, and (3) to evaluate the potential for ground-based spectral diagnostic measurements.

The data taken by the Cygnus instrument on PRECEDE I not only produced results of some significance but did indeed provide back-up to the payload photometers which operated in the visible spectral region; the cover-removal for the photometer system having failed, all photometers were rendered inoperative.

The Cygnus spectrograph, and indeed other ground based instruments, documented a quite unexpected phenomenon on PRECEDE I which could not have been detected from the payload instruments. An unpredicted plume of light trailed out behind the second-stage booster rocket. The second-stage booster had been deliberately left attached to the payload to improve vehicle neutralization characteristics.

The plume of light is now believed to be due to chemiluminescent radiation produced by the aluminum in the residual rocket fuel reacting with atomic oxygen at high altitudes to produce AlO.

The overall results achieved by the Cygnus instrumentation on PRECEDE I led DNA and AFGL to develop a second ground-based image-intensified spectrograph with greatly improved characteristics. This instrument was called Super Cygnus. Spectral resolution was improved by a factor of 10 and sensitivity by a factor of 20 while maintaining approximately the same wavelength coverage. A brief summary of its more important features is given in Table 4-2. A detailed diagram of the instrument is shown in Figure 4-4. The instrument development is described in Reference 1.

Table 4-2. Summary of Instrumentation Characteristics—Super-Cygnus Spectrograph

Parameter	Final Characteristics
Wavelength Coverage	4200 Å - 7500 Å
Linear Dispersion	14 Å/mm - 25 Å/mm
Wavelength Resolution	1 Å
Relative Aperture	f/1.5
Field of View (variable)	0.5 - 2.0°
Image Intensifier	3 stage electrostatic
Radiant Power Gain	75,000
Cathode Response	S-20 VR
Phosphor Screen	P-11
Film Size	70 mm × 125 ft
Exposure Times (Optional)	1, 2, 5, 10, 20 sec

Super Cygnus employs an echelle diffraction grating to obtain the high dispersion necessary to higher resolution. It does this at the expense of working at high diffraction orders (diffraction orders from 30 to 52) all of which would normally overlap in the image plane. A plane grating with its rulings crossed at right angles to those of the echelle is used to separate and displace the 22 diffraction orders.

Significant improvements were made in sensitivity by using a larger diameter objective lens and by developing a film transport mechanism which brings the film directly in contact with the output fiber optic face-plate of the three-stage image intensifier tube. The Cygnus instrument used relay-optic lenses to image the output fiber optic faceplate onto the film plane of a camera.

1. Tuttle, A.H. (1977) Development of a High-Resolution Image Intensified Spectrograph; DNA 4408F.

The Super Cygnus spectrograph as employed on PRECEDE II operated in the objective (that is, slitless) mode (as was the Cygnus instrument on PRECEDE I). In the slitless mode the source itself becomes the slit of the instrument. The reason for operating spectrographs in this mode is to obviate the almost impossible feat of tracking a fast moving point-like target such that its image would fall on the slit of a spectrograph.

2.2 Ultraviolet Cygnus Spectrograph

The $N_2(A^3\Sigma)$ state of excited molecular nitrogen is thought to be a potential contributor to the upper atmosphere chemistry which produces IR effects. A good handle on the abundance of molecules in the $N_2(A^3\Sigma)$ state, their altitude dependence and quenching rates could be obtained from quantitative spectra of the N_2 Vegard-Kaplan band system.

The Vegard-Kaplan band system represents forbidden transitions from the metastable $N_2(A^3\Sigma)$ state and the ground state of the nitrogen molecule. Since all the strong bands of the Vegard-Kaplan system lie in the ultraviolet any attempt to measurement would require ultraviolet sensitive instruments.

The potential importance of information on the $N_2(A^3\Sigma)$ state to the EXCEDE Program is such that AFGL concluded an attempt should be made to perform measurements of the Vegard-Kaplan bands with ground based instrumentation on the PRECEDE II event.

Electron-beam dosed air emits a strong second positive nitrogen spectrum $N_2(2P)$ throughout the same ultraviolet spectral region occupied by the Vegard-Kaplan band system. To distinguish individual bands of the two band systems requires that a spectrograph be used rather than filtered photometers.

AFGL and HSS concluded that a low-budget ultraviolet image-intensified spectrograph could be developed for PRECEDE II by marrying several optical components on hand at AFGL with the image-intensifier/camera section of the Cygnus instrument. The components available from AFGL were:

- (a) Nye Ultraviolet Telephoto Lens 150 mm f/. 1, f/1.5,
- (b) B&L Reflectance Grating 300 gr/mm, blaze wavelength 5000 Å,
- (c) Bendix Ultraviolet Proximity Focused Wafer Diode Image Intensifier.

The new instrument concept was as follows. The front end of the Cygnus spectrograph would be removed leaving only the three-stage image-intensifier tube, the relay optics, and the camera recording section. The ultraviolet diode intensifier would then be butted to the three-stage intensifier thus converting the latter tube into an ultraviolet sensitive four-stage intensifier. (Note the diode intensifier had very little gain, about a factor of 4, in comparison to the three-stage intensifier which has a radiant power gain of 40,000.) Ahead of the diode image-intensifier

would be placed the Nye lens, then the diffraction grating and a mirror flat to fold the optical system into a convenient configuration.

After the development program got underway, several problems arose with the planned approach. First, the diode image-intensifier proved to be defective and could not be made to operate. Secondly, calculations showed that a grating, blazed for 5000 Å when operated in the spectral region from 3000 Å to 4000 Å, would be very inefficient. Thirdly, a 300 gr/mm grating would give inadequate separation of the Vegard-Kaplan and Second Positive band systems.

Time and budget did not permit replacement of the diode image-intensifier. Both grating problems were solved by purchasing a 600 gr/mm diffraction grating from JACO which was blazed for 4000 Å.

An expedient, although unsatisfactory solution to the ultraviolet conversion problem was found by coating the front end of the three-stage image-intensifier with sodium salicylate. Normally sodium salicylate is used in the far ultraviolet to convert those radiations to visible radiations. In the spectral region from 3000 Å to 4000 Å where it was needed for the PRECEDE II instrument, a heavy coating thickness is required to absorb the ultraviolet. The heavy coating then acts as a diffuser which significantly degrades the image resolution.

A summary of the instrument characteristics of the Ultraviolet Cygnus Spectrograph is given in Table 4-3; more details are provided in Table 4-7.

Table 4-3. Summary of Instrument Characteristics—
Cygnus Spectrograph

Parameter	Final Characteristics
Wavelength Coverage	2900 Å - 6000 Å
Linear Dispersion	142 Å/mm
Wavelength Resolution	6 Å
Relative Aperture	f/1.5
Field of View (variable)	2.0°
Image Intensifier	3-stage electrostatic
Radiant Power Gain	40,000
UV Sensitizer	Sodium Salicylate
Cathode Response	S-20 VR
Phosphor Screen	P-11
Film Size	35 mm × 100 ft
Exposure Times (Optional)	1, 2, 5, 10, 20 sec

3. MEASUREMENT RESULTS

3.1 Operation of Instruments

The two spectrographs were operated from the same instrument control unit. A predetermined exposure plan had been formulated based on the predicted flight profile of the rocket and payload. The operation sequence is given in Table 4-4.

Table 4-4. Exposure and Timing Sequence of the Super Cygnus and Ultraviolet Cygnus Spectrographs

Time Into Flight (sec)	Timing Item
0	Vehicle Launch
60	Open Shutters—Start Film Transports Frame Rate, 1 per 5 sec
106	Commence Electron Injection
110	Change Frame Rate to 1 per 10 sec
160	One 20-sec exposure
180	One 5-sec exposure
185	One 20-sec exposure
205	Change Frame Rate to 1 per 5 sec
700	Stop Film Transports

Both instruments operated in the normal fashion. The films were unloaded from the instruments and returned promptly to Bedford, Massachusetts for processing.

3.2 Super Cygnus Results

Time has not permitted more than a superficial examination of the spectral records. However, the brief examination given the Super Cygnus record does show a remarkable data content. Figure 4-1 is an illustration of the spectra obtained during the 20-sec time period surrounding apogee of the payload.

An apogee altitude of 115 km at 180 sec into the flight was predicted. Actual apogee was 102.34 km at 172 seconds. During the 20-sec exposure shown in Figure 4-1, the electron accelerator altitude varied by only 500 meters.

Spectral orders from 30 to 49 are indicated in the photograph. The actual data record shows atmospheric emissions (for example, N_2^+ (1N), $\lambda 4278 \text{ \AA}$) in the 52nd order. Instrument sensitivity is degraded toward the edges of the field and spectral orders such as 30 and 31 at the long wavelengths and 49 through 52 at the short wavelengths did not record as strongly as was hoped. Loss of sensitivity at the edges of the field is due primarily to the inherent characteristics of electrostatic image intensifiers. Some loss can also be attributed to vignetting effects in the crossed dispersion system of the instrument.

A detailed listing of all the individual atmospheric emission features thus far observed in the record will not be presented here. Many of them are indicated in Figure 4-2. The individual features belong to the following species: N_2^+ (1N), N_2^+ (Meinel), N_2 (1P), O_2^+ (1N), NII and OI.

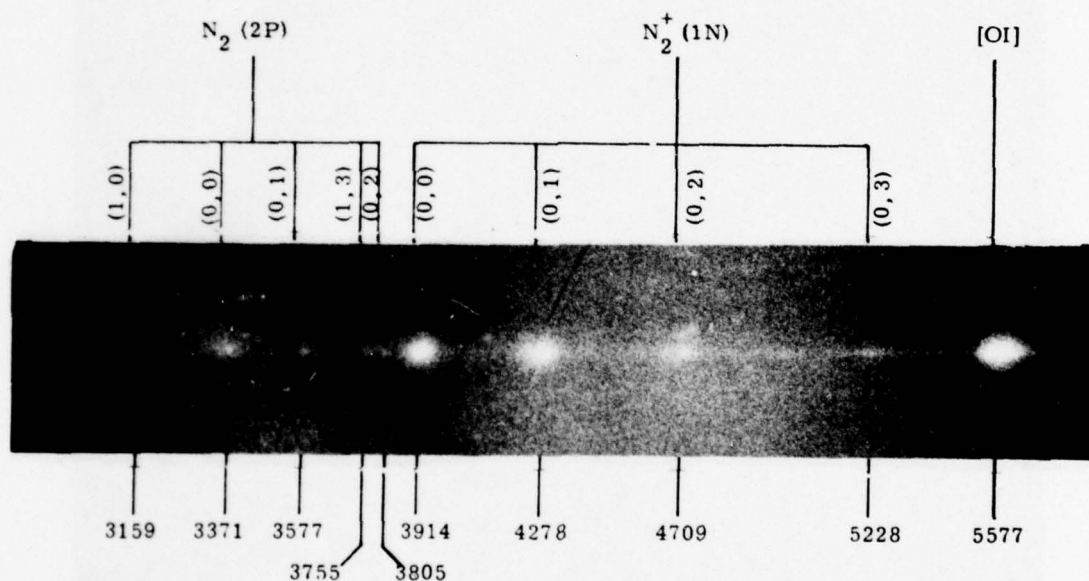


Figure 4-2. Spectrogram of PRECEDE II Event Taken With an Ultraviolet Image Intensified Spectrograph

Most of the spectral features are repeated in several diffraction orders. OI $\lambda 5577$ is an extreme case; it is seen in five orders (38 through 41). The principle order for OI $\lambda 5577$ is the 40th order as one may determine from the visual strength of the line in the photograph.

The remarkable sensitivity of the Super Cygnus instrument is clearly demonstrated by the OI $\lambda 5577$ feature. That particular OI emission is the only metastable feature which has been observed thus far in the spectrum recorded by Super Cygnus. All other emissions are fairly prompt emissions. Because the instruments are tracking the payload, any prompt emissions appear only as long as the electron deposition exists when viewed from a given aspect angle (from Southeast 70 Site the electron deposition column was viewed nearly end-on). On the other hand a long duration phenomenon (OI $\lambda 5577$ has a natural, unquenched, decay time of 0.7 sec) appears as a trail extending behind the tracked payload. The extent of the trail is of course dependent on the decay time of the metastable feature, the quenching rate and the sensitivity of the recording instrument.

The length of the OI $\lambda 5577$ afterglow as measured on the data record equated to 1.2 km at the apogee point. This length is somewhat foreshortened by geometric factors which when applied will produce an even longer trail length.

The payload velocity at apogee was approximately 300 m per second. We can thus equate the 1.2 km with about 4 sec of afterglow. This would imply 5.7 e-foldings at the natural lifetime of 0.7 seconds. Realistically, quenching of the OI $\lambda 5577$ radiation must be taken into account. In fact, the quenching rate can be recovered when quantitative data reduction techniques are applied to the records.

A summary of the quick-look visual observations of the data content of the records is given in Table 4-5. The table is more or less self-explanatory. Suffice it to call attention to two unexpected phenomena.

The first of the unexpected phenomena which were observed is the weak continuum spectra beginning at about 105 sec into the flight. The electron accelerator attempted to turn on at 106 sec and our first thoughts were to connect the continuum emissions with the accelerator. Several arguments weigh against such a correlation: (1) the accelerator turn-on attempts at this low altitude (80 km) were extremely brief and sporadic, (2) No OI $\lambda 5577$ feature is observed similar to that at comparable altitudes on the down leg of the flight, and (3) no discrete atmospheric emission features are observed in the spectrum.

R. O'Neil points out that he observes a faint afterglow trailing behind the rocket/payload in this altitude regime on image-orthicon records taken from the GEODSS site by MIT Lincoln Laboratory personnel. He tentatively ascribes this afterglow to small amounts of residual fuel escaping from the rocket and reacting with the atomic oxygen at these altitudes. The Super Cygnus spectrum would tend to confirm that the phenomenon is chemiluminescent in nature and in all probability has its origin in the manner described by O'Neil.

Table 4-5. Summary of Data Content Super Cygnus Event Film

PROJECT PRECEDE II				SUMMARY OF DATA CONTENT					HSS INC Bedford, Mass 13 Feb 1978	
Event Date: 12 Dec '77				SUPER CYGNUS EVENT FILM						
Location: WSMR										
Film No: 1753										
Frame No.	Exp. Duration (sec)	Time Into Flight (sec)	Approx. Altitude (km)	VISUAL OBSERVATIONS FROM FILM						
				N ₂ ⁺ (IN)	OI 5577	N ₂ (IP)	O ₂ ⁺ (IN)	NII	SOURCE	
E20	5	215-220	93-91	VW	S	M	M	---	E-Beam	
E21	5	220-225	91-89	VW	S	M	M	---	E-Beam	
E22	5	225-230	89-86	VW	S	M	M	---	E-Beam*	
E23	5	230-235	86-83	VW	S	M	M	---	E-Beam	
E24	5	235-240	83-80	---	W	---	---	---	E-Beam	
E25	5	240-245	80-77	---	W	VVW	VVW	---	E-Beam	
E26	5	245-250	77-73	---	W	VVW	VVW	---	E-Beam	
E27	5	250-255	73-69	---	VVW	---	---	---	E-Beam	
E28	5	255-260	69-65	---	VVW	VVW	---	---	E-Beam	
E29	5	260-265	65-61	---	VVW	VVW	---	---	E-Beam	
E30	5	265-270	61-56	---	VVW	---	---	---	E-Beam	
E31	5	270-350	61-14	---	---	---	---	---	None	
Post Event										
ST1-ST20	()	---	1.2						Star Rigel	
ST21-38	()	---	1.2						Star Gamma Pegasus	

Table 4-5. Summary of Data Content Super Cygnus Event Film

PROJECT PRECEDE II				SUMMARY OF DATA CONTENT					HSS INC Bedford, Mass 13 Feb 1978	
Event Date: 12 Dec '77				SUPER CYGNUS EVENT FILM						
Location: WSMR										
Film No: 1753										
Frame No.	Exp. Duration (sec)	Time Into Flight (sec)	Approx. Altitude (km)	VISUAL OBSERVATIONS FROM FILM						
				N ₂ ⁺ (IN)	OI 5577	N ₂ (IP)	O ₂ ⁺ (IN)	NII		
E20	5	215-220	93-91	VW	S	M	M	---	E-Beam	
E21	5	220-225	91-89	VW	S	M	M	---	E-Beam	
E22	5	225-230	89-86	VW	S	M	M	---	E-Beam	
E23	5	230-235	86-83	VW	S	M	M	---	E-Beam	
E24	5	235-240	83-80	---	W	---	---	---	E-Beam	
E25	5	240-245	80-77	---	W	VVW	VVW	---	E-Beam	
E26	5	245-250	77-73	---	W	VVW	VVW	---	E-Beam	
E27	5	250-255	73-69	---	VVW	---	---	---	E-Beam	
E28	5	255-260	69-65	---	VVW	VVW	---	---	E-Beam	
E29	5	260-265	65-61	---	VVW	VVW	---	---	E-Beam	
E30	5	265-270	61-56	---	VVW	---	---	---	E-Beam	
E31	5	270-350	61-14	---	---	---	---	---	None	
Post Event										
ST1-ST20	()	---	1.2						Star Rigel	
ST21-38	()	---	1.2						Star Gamma Pegasus	

Table 4-5. Summary of Data Content Super Cygnus Event Film (Cont)

PROJECT PRECEDE II				SUMMARY OF DATA CONTENT				HSS INC			
Event Date: 12 Dec '77								Bedford, Mass			
Location: WSMR								13 Feb 1978			
Film No: 1753											
Frame No.	Exp. Duration (sec)	Time Into Flight (sec)	Approx. Altitude (km)	VISUAL OBSERVATIONS FROM FILM						SOURCE	
				N ₂ ⁺ (IN)	OI 5577	N ₂ (IP)	O ₂ ⁺ (IN)	NII			
Pre-Event											
CO-C18	()	---	1.2							Hg-Ar Lamp Cal.	
C19-C29	()	---	1.2							Hg-Ar Lamp Cal.	
SO-S9	()	---	1.2							Star Rigel	
S-10	()	---	1.2							Star Rigel	
S11-S13	()	---	1.2							Star Rigel	
S14-S34	()	---	1.2							Rigel W/tracker Motion	
Event											
E0-E8	5	60-105	43-81	---	---	---	---	---	---	none	
E9	5	105-110	81-84	---	---	---	---	---	---	very weak continuum	
E10	10	110-120	84-90	---	---	---	---	---	---	weak continuum	
E11	10	120-130	90-94	---	---	---	---	---	---	weak continuum	
E12	10	130-140	94-98	W	VVS	S	M	W	W	E-Beam	
E13	10	140-150	98-100	W	VVS	S	M	W	W	E-Beam	
E14	10	150-160	100-102	W	VVS	S	M	W	W	E-Beam	
E15	20	160-180	102-102	M	VVS	VS	S	M	M	E-Beam	
E16	5	180-185	102-101	W	VVS	S	M	VW	VW	E-Beam	
E17	20	185-205	101-97	S	VS	S	S	M	M	E-Beam	
E18	5	205-210	97-95	VW	S	M	M	---	---	E-Beam	
E19	5	210-215	95-93	VW	S	M	M	---	---	E-Beam	

See last page of this table for legend

The second unexpected phenomenon is the persistence of the OI $\lambda 5577$ radiations to an altitude of near 60 km on the downward leg of the flight. The implication here is that the OI (1S) upper level state of $\lambda 5577$ radiation is created by electron recombination with the O_2^+ which is created by the electron beam, rather than by other processes which can take place at higher altitudes.

3.3 Ultraviolet Cygnus Results

Because of the low apogee (102.34 km rather than 115 km) the Vegard-Kaplan bands were heavily quenched. A preliminary survey of the UV Cygnus spectrum obtained at the time of apogee shows no visual indication of those bands (see Figure 4-2). The spectrum is dominated by $N_2(2P)$ and $N_2^+(1N)$ band emission features. The spectrum also includes the OI $\lambda 5577$ line emission.

A final determination of the presence or absence of the Vegard-Kaplan band system must await microdensitometer analysis of the record. Unfortunately, the image quality of the Cygnus record suffers severely from the use of an ultraviolet sensitizer as previously explained (and from flare which seems to be of a trait of the Nye ultraviolet telephoto lenses).

A quick-look summary of visual observations of the data content of the film record is given in Table 4-6.

3.4 WSMR Photographic Results

A small but extensive coverage of the PRECEDE II event had been worked out by R. O'Neil and WSMR personnel. HSS Inc. will not attempt to review the planned coverage here. We shall treat only very briefly the results of that effort.

Contrary to the usually very high success rate WSMR achieves with their cameras and tracking mounts, the WSMR photo effort on PRECEDE II suffered from extensive camera failures, film transport defects, and tracking mount problems. Only one good record was obtained by WSMR, from a camera located on the tracking mount at Southeast 70 site. This was the same tracking mount on which the AFGL telephotometers and HSS Inc. spectrographs were mounted.

The 35 mm cine camera was equipped with a very long focal length lens (104 in.) with moderate aperture ($f/8$). The camera was operated at its lowest framing rate (6 frames per sec) and had an exposure time of $1/20$ sec at that framing rate. Eastman Kodak 2484 high speed recording film was employed in the camera.

A record was obtained over a fairly extensive portion of the time that the electron accelerator was active. An example of the data obtained is shown in a sequence of frames taken near the time of payload apogee.

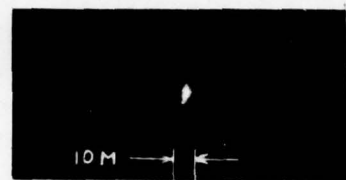
The accelerator was programmed to have an on-time of 4 sec with 2-sec intervals between pulses. The sequence of pictures shown in Figure 4-3 show every other frame of the record during the on-time of the accelerator.

Table 4-6. Summary of Data Content UV Cygnus Event Film

PROJECT PRECEDE II				SUMMARY OF DATA CONTENT				VISUAL OBSERVATIONS FROM FILM				HSS INC. Bedford, Mass 13 Feb. 1978	
Event Date: 12 Dec '77				UV CYGNUS EVENT FILM									
Location: WSMR													
Film No: 1752													
Frame No.	Exp. Duration (sec)	Time Into Flight (sec)	Approx. Altitude (km)	N ₂ ⁺ (IN)	OI 5577	N ₂ (2P)	N ₂ (VK)	Conti-num	SOURCE				
Pre-Event													
CO-C6	()	---	1.2						Hg-Ar Lamp				
C8-C19	()	---	1.2						Hg-Ar Lamp				
C21-C91	()	---	1.2						Hg-Ar Lamp				
C93-C105	()	---	1.2						Hg-Ar Lamp				
SO-S9	()	---	1.2						Star Rigel				
S11	()	---	1.2						Star Rigel				
S13-S23	()	---	1.2						Star Rigel				
S25-S26	()	---	1.2						Star Rigel				
Event													
EO-E8	5	60-105	43-81	---	---	---	---	---	Star Background				
E9	5	105-110	81-84	---	---	---	---	VW	Rocket Fuel				
E10	10	110-120	84-90	---	---	---	---	W	Rocket Fuel				
E11	10	120-130	90-94	---	---	---	---	W	Rocket Fuel				
E12	10	130-140	94-98	S	VS	M	---	---	E-Beam				
E13	10	140-150	98-100	S	VS	M	---	---	E-Beam				
E14	10	150-160	100-102	S	VS	M	?	---	E-Beam				
E15	20	160-180	102-102	VS	VS	W	?	---	E-Beam				
E16	<1	180	102	VS	VS	W	---	---	E-Beam				

Table 4-6. Summary of Data Content UV Cygnus Event Film (Cont)

PROJECT PRECEDE II				SUMMARY OF DATA CONTENT				HSS INC. Bedford, Mass 13 Feb. 1978			
Event Date: 12 Dec '77				UV CYGNUS EVENT FILM							
Location: WSMR											
Film No: 1752											
Frame No.	Exp. Duration (sec)	Time Into Flight (sec)	Approx. Altitude (km)	VISUAL OBSERVATIONS FROM FILM						SOURCE	
				N ₂ ⁺ (IN)	OI 5577	N ₂ (2P)	N ₂ (VK)	Continuum			
E17	5	180-185	102-101	VS	VS	M	?	---	---	E-Beam	
E18	1	185	101	VS	VS	W	---	---	---	E-Beam	
E19	20	185-205	101-97	VS	VS	M	?	---	---	E-Beam	
E20	1	205	97	VS	S	W	---	---	---	E-Beam	
E21	5	205-210	97-95	S	S	M	---	---	---	E-Beam	
E22	5	210-215	95-93	S	S	M	---	---	---	E-Beam	
E23	5	215-220	93-91	S	S	M	---	---	---	E-Beam	
E24	5	220-225	91-89	S	S	M	---	---	---	E-Beam	
E25	5	225-230	89-86	S	S	W	---	---	---	E-Beam	
E26	5	230-235	86-83	S	S	W	---	---	---	E-Beam	
E27	5	235-240	83-80	M	M	VW	---	---	---	E-Beam	
E28	5	240-245	80-77	M	M	VW	---	---	---	E-Beam	
E29	5	245-250	77-73	M	M	VW	---	---	---	E-Beam	
E30	5	250-255	73-69	---	---	---	---	---	---	E-Beam	
E31	5	255-260	69-65	M	VW	VW	---	---	---	E-Beam	
E32	5	260-265	65-61	M	---	---	---	---	---	E-Beam	
E33-E50	5	265-345	61-15	---	---	---	---	---	---	Star Background	
Post Event											
ST0-ST19	()	---	1.2	---	---	---	---	---	---	Star Rigel	
ST23-ST26	()	---	1.2	---	---	---	---	---	---	Star Gamma Pegasus	



05h 52m 46.8 sec UT



49.3 sec



47.3 sec



49.8 sec



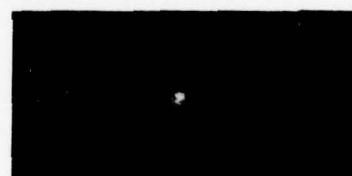
47.8 sec



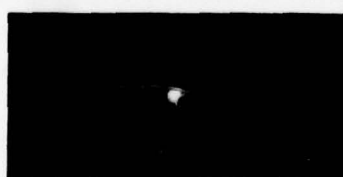
50.3 sec



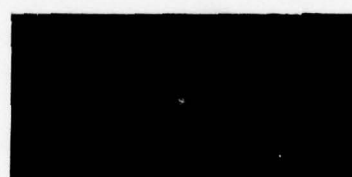
48.3 sec



50.8 sec



48.8 sec



51.1 sec

Figure 4-3. Telescopic Cine-Photographs of the PRECEDE II Event Near Payload Apogee

The electron beam deposition is seen very faintly in the photographs. The deposition column can be recognized by its behavior. The payload carrying the accelerator had a rotation rate of once per 6 seconds. During half the rotation period, the electron beam was injected up the earth's geomagnetic field. During the other half, it was aimed down the magnetic field lines. In the sequence of pictures the beam can be seen reversing its direction once during the on-pulse.

An unexplained phenomena is present in the photographs. Note first that the spatial resolution of the camera system is about 2 m (the first frame of the sequence has two vertical lines drawn in to show the equivalent of 10 m at the payload). A bright object, equivalent in approximate size to the resolution limit, is apparent in the photographs. Slight stepping motions of the tracking mount make the object appear to have length in some of the frames. Real length should not be ascribed to the object at these times.

Two tentative explanations for the phenomena have been put forth thus far: (1) a portion of the electron beam returns to the vehicle and causes a fluorescence of the skin, and (2) the object is in reality the first few meters of electron beam deposition where the electron density (and therefore atmospheric excitation) is much greater than when the beam expands to its full diameter of approximately 20 meters.

If the latter situation is the case, one must ponder the possible avenues this opens up for conceivably remarkable improvements in ground-based spectroscopic measurements using large aperture long-focal-length image-intensified instruments.

4. CONCLUSIONS AND RECOMMENDATIONS

4.1 Conclusions

PRECEDE II Event was the first opportunity to exercise the Super Cygnus spectrograph on the EXCEDE program. The instrument performed well in most respects. Its sensitivity in the central portion of its recording field appears to live up to predictions. The fall-off in sensitivity toward the edges of the field causes some concern.

The instrument was adjusted such that diffraction order 38 fell in the center of the field. Under these circumstances the N_2^+ (Meinel) bands in the 30th and 31st orders, and the N_2^+ (1N) band at 4278 \AA in the 52nd order appeared at the edges of the field. Both features are important to a knowledge of the excitation and de-excitation processes of the upper atmosphere (as well as all the features in the intervening spectral region).

The 4278 \AA N_2^+ (1N) band was recorded only weakly. Other bands in the $0, v''$ progression, (for example, at 4709 \AA and 5288 \AA) which recorded more strongly, will serve to replace the 4278 \AA band in the analysis of the spectra. Only one band the (3,0) transition of the N_2^+ (Meinel) system was recorded with adequate density to permit radiometric analysis.

The N_2 (1P) and O_2^+ (1N) band systems recorded remarkably well. There should be no problems performing a radiometric analysis of their features. The OI 5577 \AA auroral transition was so strong it should present a wealth of altitude dependent information.

Depending upon DNA/AFGL priorities and interests, many other features recorded by the Super-Cygnus spectrograph can be subjected to radiometric analysis; for example, the continuum spectra at early times (which possibly represents a chemiluminescent reaction of rocket fuel with atomic oxygen); the rotational structure of the N_2^+ (1N) bands at 4709 \AA and 5228 \AA which may yield a temperature determination.

The Super Cygnus spectrograms have been only superficially analyzed to date. Thorough analysis may well yield other information of value to the EXCEDE program. A comprehensive analysis will start with microdensitometer scans and include radiometric calibrations, sensitometry, and computer plotting leading to a final empirical analysis of the data.

The results of the Ultraviolet Cygnus spectrograph are dissappointing. Diffusion of the image in the ultraviolet sensitizer coating on the image-intensifier tube and flare light in the Nye lens caused the instrument to have poor spectral resolution.

The low apogee of the payload caused the Vegard-Kaplan bands to be severely quenched; this combined with the poor resolution may prove to be the cause of a possible failure to record that band system. A final determination on the recording of the Vegard-Kaplan bands by the Ultraviolet Cygnus instrument must await the application of image-enhancement techniques in the data reduction process.

4.2 Recommendations

Ground-based optical diagnostics on EXCEDE Events had their origin in the need to provide certain types of information which would be virtually impossible to obtain from the payload itself and as a back-up to those payload instruments which operate in spectral regions which are accessible through the atmospheric windows from ground stations.

The investment in equipment development has been modest as the feasibility, information content, and quality of data have been explored. Whenever possible AFGL has utilized existing optical systems to augment the recording of the events (for example, Cloudcroft, GEODDS Stations).

On its part, HSS Inc. has concentrated on developing image-intensified spectral systems. Such systems offer great potential, for in principle they are the equivalent of a photomultiplier tube operating at each pixel of spatial resolution and are limited only by the night sky background level in that pixel.

The spectrographs developed to date have not approached the limit that can be predicted for ground based instruments. Super Cygnus demonstrated a marked improvement in sensitivity over the original Cygnus instrument. But it has limitations inherently due to certain of the low-cost and on-hand optical components used in its construction. Nor does it provide the full range of wavelength coverage accessible through atmospheric windows with high-gain photo-emissive sensors limited in sensitivity only by photon noise of the sky background.

The limit of ground based instrumentation will be reached when objective focal lengths are such that a pixel of spatial resolution is just exceeded by the dimensions of the electron beam deposition and simultaneously when there is sufficient telescope aperture and intensifier gain to just record the night sky background at exposure times equivalent to the pulse duration of the electron accelerator.

In that direction, HSS Inc. recommends for consideration on future EXCEDE events several possible improvements and changes in ground-based spectral instrumentation. These suggestions are as follows:

(a) Modification of Super Cygnus Spectrograph

1. Replace existing 300-mm, $f/3$ objective lens with a 600-mm to 1000-mm $f/3$ objective lens.
2. Replace Super Farron Camera lens with an equivalent lens having better transmission at 4200 Å.
3. If feasible, within the confines of the present instrument housing, replace the three-stage electrostatic image intensifier tube with a three-stage magnetic intensifier tube to provide uniformity of sensitivity across the field, no geometric (pin cushion) distortion and added sensitivity.
4. Utilize 4XN film rather than 2484 film for improved sensitivity and resolution; 4XN film is not available in 70 mm size except on special order.

(b) Develop Improved Ultraviolet Image-Intensified Spectrograph

1. Utilize a three-stage ultraviolet sensitive magnetically-focused image intensifier tube (the equivalent electrostatically focused tube is not available because a fiber optics face plate at the cathode end of the tube is required and no-one has yet developed an ultraviolet transmitting fiber optic face plate).

2. Utilize an ultraviolet optical system which will have an effective focal length of 300 mm (to make the electron beam deposition column of 20 m equivalent to a pixel of information).
3. Utilize a film transport mechanism which places the film in contact with the fiber optic output of the image-intensifier tube to avoid the factor of five loss in light inherent in the best possible (f/1.0) relay optics, as is done in the Super Cygnus instrument.

(c) Develop a Dedicated $N(^2D)$ Spectrometer

The population of (^2D) state of NI in upper atmospheric chemistry seems to be a dominate consideration. Yet a direct measurement of the radiations from the $(^2D - ^4S)$ transition which can lead to a measure of the population has not been attempted. The difficulties are enormous: the transition produces two lines at 5200.7 Å and 5198.5 Å which reside within the rotational structural of the $N_2^+ 5228$ Å band. Intensities of those rotational lines dwarf the $N(^2D)$ radiations which are extremely weak because of the 26-hr lifetime of that state.

There is little advantage to be gained by using a payload instrument and a significant number of advantages to a ground based measurement of the $(^2D - ^4S)$ radiations. (A relative comparison of the methods is too lengthy a subject and is avoided here.) With the 100-kW accelerator powers now contemplated, we believe the tools are near at hand for a realistic attempt at this difficult measurement. A design analysis would indicate the optimum approach, but the skeleton outlines are obvious. Very high spectral dispersion with limited wavelength coverage are dictated along with an extremely sensitive night-sky-background limited image-intensified recording system. Multi-channel recording is essential (that is, scanning of the spectrum should be avoided so that maximum exposure at each element of wavelength resolution is achieved). The instrument should also take advantage of the fact that the $N(^2D)$ radiations persist long after the payload has left a dosed region of its trajectory.

Our final recommendation concerns the not-as-yet understood results of the WSMR 104-in. telescopic camera. A real effort should be made to explain the origin of the high brightness core in the recorded image. If the explanation should prove to have its origin in atmospheric emissions from the narrow region of the electron beam, then ground-based instruments can take the ultimate approach to the sensitivity of payload instruments in those spectral regions accessible through the atmosphere.

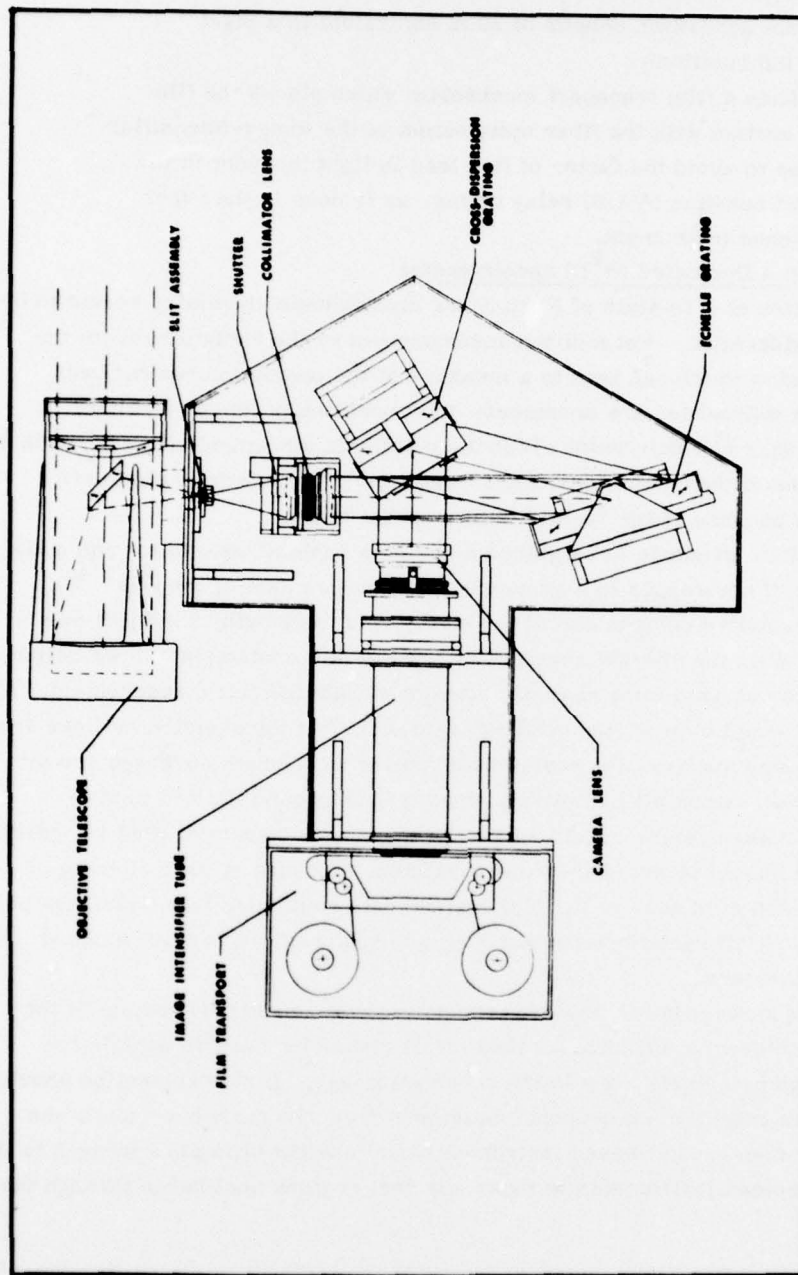


Figure 4-4. Optical Diagram of the Super Cygnus Spectrograph

Table 4-7. Characteristics of the Ultraviolet Image-Intensified
Cygnus Spectrograph

<u>SPECTRAL FEATURES</u>	
Wavelength Coverage (nominal)	2900 Å - 6000 Å
Linear Dispersion (nominal)	142 Å/mm
Grating Rulings	590 g/mm
Wavelength Resolution	6 Å
<u>OPTICAL FEATURES</u>	
Configuration	Objective
Objective Lens	NYE
(a) f/n	F/1.5
(b) f.l.	150 mm
Field-of-View	+ 0.5°
Resolution (Image Tube)	
(a) Center	12 lines/mm
(b) Edge	10 lines/mm
<u>ELECTRONIC FEATURES</u>	
Image Intensifier	VARO 8606 (ABC)
(a) Type (electrostatic)	3-Stage
(b) Cathode Response	S-20VS
(c) UV Sensitizer	1 mg/cm ² Sodium Salicylate
(d) Screen, Phosphor	P-11
(e) Radiant Power Gain	40,000
(f) End Plages	Flat; fiberoptic
<u>RECORDING FEATURES</u>	
Camera Type	Flight Research IVC
Film Size	35 mm × 100 ft
Format Size	20.4 mm × 18.6 mm
Shutter Mode	Open to Open
Shutter Sector Opening	130°
Shutter Program Options	10, 5, 2, 1, 0.5, 0.2, 0.1, 0.05, fps
Film Type	4XN

5. Conclusions

R.R. O'Neil
Radiation Effects Branch
Optical Physics Division
Air Force Geophysics Laboratory
Hanscom AFB, Massachusetts 01731

1. CONCLUSIONS

A preliminary review of the results of the PRECEDE II launch from the White Sands Missile Range on 13 December 1977 indicates:

(a) The prototype electron accelerator module planned for the EXCEDE II experiment successfully endured a severe engineering test during the PRECEDE II launch,

(b) The rocketborne short wave infrared interferometer, using liquid nitrogen cooled optics and detector, functioned with some loss in modulation efficiency due to optical misalignment during the powered rocket boost period. The principal problem area to be addressed prior to the EXCEDE II experiment is redesign of the monochromatic reference source. The interferometer was successfully recovered from the PRECEDE II launch with little apparent damage to the optical or electronic components,

(c) The numerous ground based optical systems readily recorded the ultra-violet and visible emissions induced in the night sky by the 20 kW electron source. The prospect of higher power electron accelerators operating at altitudes up to 120 km, where metastable species [$N(^2D)$, $N_2(A^3\Sigma)$, $O(^1S)$, $O(^1D)$, ...] are less

severely collisionally deactivated, offers the potential to determine atmospheric production and loss mechanisms for a many excited species of aeronomic interest for their precursor role in infrared atmospheric emissions. The ground based measurement capability may be improved by the fabrication of new instrumentation or by modifying existing instrumentation to optimize their measurement capabilities in support of an artificial auroral experiment.

DNA DISTRIBUTION LIST

DEPARTMENT OF DEFENSE

Director
Defense Advanced Rsch Proj Agency
Architect Building
1400 Wilson Blvd.
Arlington, VA 22209
ATTN: STD
ATTN: LTC W.A. Whitaker
ATTN: LTC William Cuneo
ATTN: Stephen Zakany

Defense Documentation Center
Cameron Station
Alexandria, VA 22314
2 cy ATTN: TC

Director
Defense Nuclear Agency
Washington, DC 20305
ATTN: TISI Archives
3 cy ATTN: TITL Tech. Library
ATTN: RAEV, Harold C. Fitz, Jr.
3 cy ATTN: RAAE, Charles A. Blank
ATTN: RAAE, Maj. R. Bigoni
ATTN: RAAE, Maj. J. Mayo
ATTN: DDST

Commander
Field Command
Defense Nuclear Agency
Kirtland AFB, NM 87115
ATTN: FCPR

Chief
Livermore Division Fld. Command DNA
Lawrence Livermore Laboratory
P.O. Box 808
Livermore, CA 94550
ATTN: FCPRL

Under Secy. of Def. for Rsch. & Engrg.
Department of Defense
Washington, DC 20301
ATTN: S&SS(OS)

DEPARTMENT OF THE ARMY

Commander/Director
Atmospheric Sciences Laboratory
U.S. Army Electronics Command
White Sands Missile Range, NM 88002
3cy ATTN: DELAS-AF-M, F.E. Niles
3cy ATTN: H. Ballard

DEPARTMENT OF THE ARMY (Cont)

Director
BMD Advanced Tech Ctr.
Huntsville Office
P.O. Box 1500
Huntsville, AL 35807
ATTN: ATC-O, W. Davies
ATTN: ATC-T, M. Capps

Commander
Harry Diamond Laboratories
2800 Powder Mill Road
Adelphi, MD 20783
(CNWDI-Inner Envelope:
ATTN: D-EL40-BBH)
2 cy ATTN: DELHD-NP, F. H. Wimenitz

Commander
U.S. Army Nuclear Agency
7500 Backlick Road
Building 2073
Springfield, VA 22150
ATTN: MONA-WE

Deputy Chief of Staff for Rsch. Dev. & Acq.
Deputy of the Army
Washington, D.C. 20310
ATTN: NCB Division
ATTN: DAMA-CSZ-C
ATTN: DAMA-WSZC

Director
U.S. Army Ballistic Research Labs.
Aberdeen Proving Ground, MD 21005
ATTN: John Mester

Commander
U.S. Army Electronics Cmd
Fort Monmouth, NJ 07703
ATTN: Inst. for Expl. Rsch.
5 cy ATTN: DRSEL
ATTN: Stanley Kronenberger
ATTN: Weapons Effects Section

Commander
U.S. Army Foreign Science & Tech Ctr.
220 7th Street, NE
Charlottesville, VA 22901
ATTN: Robert Jones

Chief
U.S. Army Research Office
P.O. Box 12211
Triangle Park, NC 27709
2 cy ATTN: Robert Mace

DEPARTMENT OF THE NAVY

Commander
Naval Ocean Systems Center
San Diego, CA 92152
ATTN: Code 2200, Ilan Rothmuller
ATTN: Code 2200, Richard Pappert
ATTN: Code 2200, William Moler
ATTN: Code 2200, Jurgen Richter
ATTN: Code 2200, Herbert Hughes

Director
Naval Research Laboratory
Washington, DC 20375
ATTN: Code 7750, Darrell F. Strobel
ATTN: Code 7127, Charles Y. Johnson
ATTN: Code 7701, Jack D. Brown
ATTN: Code 7750, Paul Julienne
ATTN: Code 7709, Wahab Ali
ATTN: Code 7700, Timothy P. Coffey
ATTN: Code 7750, J. Davis
ATTN: Code 2600, Tech. Lib.
ATTN: Code 7712, Douglas P. McNutt
ATTN: Code 7750, S. Ossakon
ATTN: Code 7750, J. Fedder

Officer-in-Charge
Naval Surface Weapons Center
White Oak, Silver Springs, MD 20910
ATTN: Code WA501, Navy Nuc.
Prgms. Office
ATTN: Tech. Library

Superintendent
Naval Postgraduate School
Monterey, CA 93940
ATTN: Tech. Rpts. Librarian

Commander
Naval Intelligence Support Center
4301 Suitland Rd.
Washington, DC 20390
ATTN: Doc. Con.

DEPARTMENT OF THE AIR FORCE

AF Geophysics Laboratory, AFSC
Hanscom AFB, MA 01731
10 cy ATTN: LKB, K.S.W. Champion
ATTN: OPR, Alva T. Stair
ATTN: PHG, J.C. McClay
2 cy ATTN: LKO, R. Huffman
3 cy ATTN: LKD, R.S. Narcisi
2 cy ATTN: OPR-1, J. Kennealy
2 cy ATTN: OPR-1, R. Murphy
5 cy ATTN: OPR-1, J. Ulwick

DEPARTMENT OF THE AIR FORCE (Cont)

AF Weapons Laboratory, AFSC
Kirtland AFB, NM 87119
ATTN: SUL
2 cy ATTN: DYM, Maj Gary Ganong

Commander
ASD
WPAFB, OH 45433
ATTN: ASD-YH-EX,
LTC Robert Leverette

SAMSO/SZ
P.O. Box 92960
Worldway Postal Center
Los Angeles, CA 90009
(Space Defense Systems)
ATTN: SZJ, Maj Lawrence Doan

SAMSO/AW
P.O. Box 92960
Worldway Postal Center
Los Angeles, CA 90009
10 cy ATTN: AWW

AFTAC
Patrick AFB, FL 32925
2 cy ATTN: Tech. Library

Headquarters
Air Force Systems Cmd.
Andrews AFB,
Washington, DC 20331
ATTN: DLS
ATTN: DLCAW
ATTN: Tech. Library
ATTN: DLXP
ATTN: DLTW
ATTN: SDR

Hqs. USAF/RD
Washington, DC 20330
3 cy ATTN: RDQ

Commander
Rome Air Development Ctr.
Griffiss AFB, NY 13440
3 cy ATTN: J.J. Simons OCSC

U.S. ENERGY RSCH. and DEV. ADMIN.

Division of Military Application
Department of Energy
Washington, DC 20545
ATTN: Doc. Con.

U.S. ENERGY RSCH. and DEV. ADMIN. (Cont)

Los Alamos Scientific Laboratory
P.O. Box 1663
Los Alamos, NM 87545
ATTN: Doc. Con. for R.A. Jeffries
ATTN: Doc. Con. for C.R. Mehl,
Org. 5230
ATTN: Doc. Con. for H.V. Argo
ATTN: Doc. Con. for M. Tierney,
J-10
ATTN: Doc. Con. for Robert Brownlee
ATTN: Doc. Con. for William Maier
ATTN: Doc. Con. for Reference Library,
Ann Beyer

Sandia Laboratories
Livermore Laboratory
P.O. Box 969
Livermore, CA 94550
ATTN: Doc. Con. for Thomas Cook,
Org. 8000

Sandia Laboratories
P.O. Box 5800
Albuquerque, NM 87115
ATTN: Doc. Con. for W.D. Brown,
Org. 1353
5 cy ATTN: Doc. Con. for Morgan Kramma,
Org. 5720
ATTN: Doc. Con. for L. Anderson,
Org. 1247
ATTN: Doc. Con. for Frank Hudson,
Org. 1722
ATTN: Doc. Con. for Sandia Rpt. Coll.
Org. 3422-1

University of California
Lawrence Livermore Lab.
P.O. Box 808
Livermore, CA 94550
ATTN: W.H. Duewer, Gen. L-400
ATTN: Julius Chang, L-71
ATTN: G.R. Haugen, L-404
ATTN: D.J. Wuebbles, L-142

Department of Energy
Division of Headquarters Services
Library Branch F-043
Washington, DC 20545
ATTN: Doc. Con. for Class
Tech. Library

OTHER GOVERNMENT

Albany Metallurgy Research Center
U.S. Bureau of Mines
P.O. Box 70
Albany, NY 97321
ATTN: Eleanor Abshire

OTHER GOVERNMENT (Cont)

Central Intelligence Agency
ATTN: RD/SI Room 5G48
Headquarters Building
Washington, DC 20505
ATTN: NED/OSI - 2g48 Hqs.

Department of Commerce
National Bureau of Standards
Washington, DC 20234
(All correspondence: Attn: Sec Ofcer for)
ATTN: James DeVoe
ATTN: Stanley Abramowitz
ATTN: J. Cooper
ATTN: George A. Sinnott
ATTN: K. Kessler
ATTN: M. Krauss
ATTN: Lewis H. Gevantman

National Oceanic and Atmospheric
Administration
Environmental Research Laboratories
Department of Commerce
Boulder, CO 80302
ATTN: George C. Reid
3 cy ATTN: Eldon Ferguson
3 cy ATTN: Fred Fehsenfeld

Department of Transportation
Office of the Secretary
TAD-44.1, Room 10402-B
400 7th Street, S.W.
Washington, DC 20590
ATTN: Samuel C. Coronitti

NASA
Goddard Space Flight Ctr
Greenbelt, MD 20771
3 cy ATTN: A.C. Aiken
ATTN: A. Tempkin
ATTN: S.J. Bauer
ATTN: Tech. Library
ATTN: T. Siry

NASA
600 Independence Ave., S.W.
Washington, DC 20546
ATTN: A. Gessow
ATTN: D.P. Cauffman
ATTN: R. Fellows
ATTN: A. Schardt
ATTN: M. Tepper

NASA
Langley Research Ctr
Langley Station
Hampton, VA 23365
ATTN: Charles Schexnayder

OTHER GOVERNMENT (Cont)

NASA Wallops Flight Ctr
Wallops Island, VA 23337
ATTN: James W. Gray

NASA
Ames Research Center
Moffett Field, CA 94035
ATTN: Walter L. Starr
ATTN: R. Whitten
ATTN: Ilia G. Poppoff
ATTN: Neil H. Farlow

NASA
George C. Marshall Space Flight Ctr
Huntsville, AL 35812
ATTN: C.R. Balcher
ATTN: N.H. Stone
ATTN: W.A. Oran
ATTN: John Watts
ATTN: W.T. Roberts
ATTN: R.D. Hudson
ATTN: R. Chappell

DEPARTMENT OF DEFENSE
CONTRACTORS

Aerodyne Research, Inc.
Bedford Research Park
Crosby Drive
Bedford, MA 01730
ATTN: M. Camac
ATTN: F. Bien

Aerospace Corporation
P.O. Box 92957
Los Angeles, CA 90009
ATTN: R.D. Rawcliffe
ATTN: Harris Mayer
ATTN: Thomas D. Taylor
ATTN: R. Grove
ATTN: N. Cohen
ATTN: Sidney W. Cash
ATTN: T. Widhoph
ATTN: Irving M. Garfunkel
ATTN: R.J. McNeal
ATTN: Julian Reinheimer
ATTN: V. Josephson

Brown Engineering Company, Inc.
Cummings Research Park
Huntsville, AL 35807
ATTN: Ronald Patrick
ATTN: N. Passino

DEPARTMENT OF DEFENSE
CONTRACTORS (Cont)

Denver, University of
Colorado Seminary
Denver Research Institute
P.O. Box 10127
Denver, CO 80210
(Only 1 copy of Class Reports)
ATTN: Sec. Officer for
David Murcrae
ATTN: Sec. Officer for
Mr. Van Zyl

Aero-Chem Rsch. Labs, Inc.
P.O. Box 12
Princeton, NJ 08540
ATTN: A. Fortijn
ATTN: H. Pergament

Aeronomy Corporation
217 S. Neil Street
Champaign, IL 61820
ATTN: S.A. Bowhill

Avco-Everett Rsch. Lab., Inc.
2395 Revere Beach Pkwy.
Everett, MA 02149
ATTN: Tech. Library
ATTN: George Sutton
ATTN: C.W. Von Rosenberg, Jr.

Battelle Memorial Institute
505 King Avenue
Columbus, OH 43201
ATTN: Donald J. Hamman
ATTN: STOIAC
ATTN: Richard K. Thatcher

The Trustees of Boston College
Chestnut Hill Campus
Chestnut Hill, MA 02167
2 cy ATTN: Chmn Dept. of Chem.
ATTN: Chmn Dept. of Phys.

California at Riverside, Univ. of
Riverside, CA 92502
ATTN: Alan C. Lloyd
ATTN: James N. Pitts, Jr.

California at San Diego, Univ. of
3175 Miramar Rd.
LaJolla, CA 92037
ATTN: S.C. Lin

DEPARTMENT OF DEFENSE
CONTRACTORS (Cont)

General Electric Company
Space Division
Valley Forge Space Center
Goddard Blvd. King of Prussia
P.O. Box 8555
Philadelphia, PA 19101
ATTN: Robert H. Edsall
ATTN: P. Zavitsands
ATTN: T. Baurer
ATTN: M.H. Bostner
ATTN: J. Burns
ATTN: F. Alyea

General Electric Company
Tempo-Center for Advanced Studies
816 State Street (P.O. Drawer 00)
Santa Barbara, CA 93102
ATTN: Warren S. Knapp
5 cy ATTN: DASIAC
ATTN: Jay Jordano
ATTN: Tim Stephen
ATTN: Don Chandler
ATTN: B. Gambill

General Research Corporation
P.O. Box 3587
Santa Barbara, CA 93105
ATTN: John Ise, Jr.

Geophysical Institute
University of Alaska
Fairbanks, AK 99701
(All Class ATTN: Security Officer)
ATTN: T.N. Davis (Uncl. only)
3 cy ATTN: Neal Brown (Uncl. only)
ATTN: R. Parthasarathy
ATTN: B.J. Watkins
ATTN: D.J. Henderson
ATTN: J.S. Wagner

Calspan Corporation
P.O. Box 235
Buffalo, NY 14221
ATTN: C.E. Treanor
ATTN: G.C. Valley
ATTN: M.G. Dunn
ATTN: W. Wurster

California Inst. of Tech.
Jet Propulsion Lab.
4800 Oak Grove Drive
Pasadena, CA 91103
ATTN: Joseph Ajello

DEPARTMENT OF DEFENSE
CONTRACTORS (Cont)

California, Univ. of
Berkeley Campus, Rm. 318
Spoul Hall
Berkeley, CA 94720
ATTN: Harold Johnston
ATTN: F. Mozer
ATTN: W.H. Miller

California, State of
Air Resources Board
9528 Telstar Avenue
El Monte, CA 91731
ATTN: Leo Zafonte

Colorado, Univ. of
Ofc. of Contracts & Grants
370 Administrative Annex
Boulder, CO 80302
ATTN: A. Phelps
ATTN: Jeffrey B. Pearce
ATTN: C. Beaty
ATTN: C. Lineberger
ATTN: Charles A. Barth

Institute for Defense Analyses
400 Army-Navy Drive
Arlington, VA 22202
ATTN: Hans Wolfhard
ATTN: Ernest Bauer

Lockheed Missiles and Space Co., Inc.
3251 Hanover Street
Palo Alto, CA 94304
ATTN: Richard G. Johnson,
Dept 52-12
ATTN: Martin Walt, Dept. 52-10
ATTN: J.B. Reagan, D/52-12
ATTN: John R. Cladis, Dept. 52-12
ATTN: Tom James
ATTN: Billy M. McCormac,
Dept. 52-54
ATTN: John Kumer
ATTN: Robert D. Sears,
Dept. 52-14

Mission Research Corporation
735 State Street
Santa Barbara, CA 93101
ATTN: D. Archer
ATTN: R. Fischer
5 cy ATTN: D. Sowle
ATTN: M. Scheibe
ATTN: D. Sappenfield

**DEPARTMENT OF DEFENSE
CONTRACTORS (Cont)**

Columbia Univ, The Trustees
In the City of New York
LaMont Doherty Geological
Observatory-Torrey Cliff
Palisades, NY 19064
ATTN: B. Phelan

Columbia Univ, The Trustees of
City of New York
116th St. & Broadway
New York, NY 10027
ATTN: Richard N. Zare
ATTN: H. M. Foley

Cornell Univ
School of Electrical Engrg
Ithaca, NY 14850
ATTN: Michael Kelly

Concord Sciences
P.O. Box 119
Concord, MA 01742
ATTN: Emmett A. Sutton

Lowell, University of
Center for Atmospheric Rsch.
450 Aiken Street
Lowell, MA 01854
ATTN: G. T. Best

Minnesota, Univ of
2030 University Ave., S. E.
Minneapolis, MN 55414
ATTN: J. R. Winkler

Photometrics, Inc.
442 Marrett Road
Lexington, MA 02173
ATTN: Irving L. Kufsky

Physical Dynamics, Inc.
P.O. Box 1089
Berkeley, CA 94701
ATTN: Joseph B. Workman
ATTN: A. Thompson

Physical Sciences, Inc.
30 Commerce Way
Woburn, MA 01801
ATTN: Kurt Wray
ATTN: R. L. Taylor
ATTN: G. Caledonia

**DEPARTMENT OF DEFENSE
CONTRACTORS (Cont)**

R & D Associates
P.O. Box 9695
Marina Del Rey, CA 90291
ATTN: Robert F. Lelevier
ATTN: Forrest Gilmore
ATTN: Richard Latter
ATTN: R. G. Lindgren
ATTN: Bryan Gabbard
ATTN: H. A. Ory
ATTN: R. P. Turco
ATTN: Albert L. Latter
ATTN: D. Dee

R & D Associates
1401 Wilson Blvd.
Suite 500
Arlington, VA 22209
ATTN: Herbert J. Mitchell
ATTN: J. W. Rosengren

Rand Corporation
1700 Main Street
Santa Monica, CA 90406
ATTN: Cullen Crain

Physical Sciences Lab.
11007 Candlelight Lane
Potomac, MD 20354
ATTN: Warren Berning

Physics International Company
2700 Merced Street
San Leandro, CA 94577
ATTN: Doc. Con. for Tech. Lib.

Pittsburgh, Univ. of
of the CmwltH Sys. of Higher Education
Cathedral of Learning
Pittsburgh, PA 15213
ATTN: Wade L. Fite
ATTN: Manfred A. Biondi
ATTN: Frederick Kaufman
ATTN: Edward Gerjuoy

Princeton, Univ., The Trustees of
Forrestal Campus Library
Box 710
Princeton University
Princeton, NJ 08540
ATTN: Arnold J. Kelly

Science Applications, Inc.
P.O. Box 2351
La Jolla, CA 92038
ATTN: Daniel A. Hamlin
ATTN: David Sachs

DEPARTMENT OF DEFENSE CONTRACTORS
(Cont)

Space Data Corporation
1333 W. 21st Street
Tempe, AZ 85282
ATTN: Edward F. Allen

SRI International
333 Ravenswood Avenue
Menlo Park, CA 94025
ATTN: Walter G. Chestnut
ATTN: M. Baron
ATTN: Ray L. Leadabrand
ATTN: Dan McDaniels

SRI International
1611 North Kent Street
Arlington, VA 22209
ATTN: Charles Hulbert

Technology International Corporation
75 Wiggins Avenue
Bedford, MA 01730
ATTN: W. P. Boquist

United Technologies Corp.
755 Main Street
Hartford, CT 06103
ATTN: H. Michels
ATTN: Robert H. Bullis

Utah State University
P.O. Box 1357
Logan, UT 84322
3 cy ATTN: Kay Baker
3 cy ATTN: Doran Baker
ATTN: D. Burt
ATTN: C. Wyatt

Visidyne, Inc.
19 Third Avenue
North West Industrial Park
Burlington, MA 01803
ATTN: Henry J. Smith
ATTN: T. C. Degges
ATTN: William Reidy
ATTN: Charles Humphrey
ATTN: J. W. Carpenter

Wayne State Univ.
1064 Mackenzie Hall
Detroit, MI 48202
ATTN: Pieter K. Rol
ATTN: R. H. Kummier

DEPARTMENT OF DEFENSE
CONTRACTORS (Cont)

Wayne State University
Dept. of Physics
Detroit, MI 48202
ATTN: Walter E. Kauppila

Yale University
New Haven, CT 06520
ATTN: Engrg. Dept.